Published OnlineFirst June 3, 2011; DOI:10.1158/1078-0432.CCR-10-3131

form evident tumors. HT29 tumor-bearing mice were treated with i.p. injections of 125 μg figitumumab (twice a week) along with 5-FU or PBS. Although either 5-FU or figitumumab tended to suppress tumor growth, the combination therapy was much more effective than either treatment alone (Fig. 3A). Then, BxPC3 cells were inoculated in nude mice. Figitumumab monotherapy reduced the tumor growth rate of BxPC3; however, the combination with this drug and gemcitabine most effectively suppressed growth among all tested groups (Fig. 3B). However, both murine body weight and serum glucose concentration on sacrifice were not different among the 4 groups of mice.

Serum concentrations of IGF axis ligands were assessed by ELISA at the time of sacrifice. As sample number and volume were limited, we analyzed those in 2 groups, figitumumab or control ($n = 8$). Concentrations of serum IGF-I, growth hormone, insulin, and IGFBP3 were not significantly different between the 2 groups (Fig. 3C).

Resected tumor samples were investigated by immunohistochemical and TUNEL assays (Fig. 3D). The expression of IGF-IR was suppressed in BxPC3 by figitumumab monotherapy and in the both cell lines by the combination therapy. Although all treatments suppressed InsR in HT29, only the combination up-regulated InsR in BxPC3. Both 5-FU and figitumumab induced apoptosis in HT29

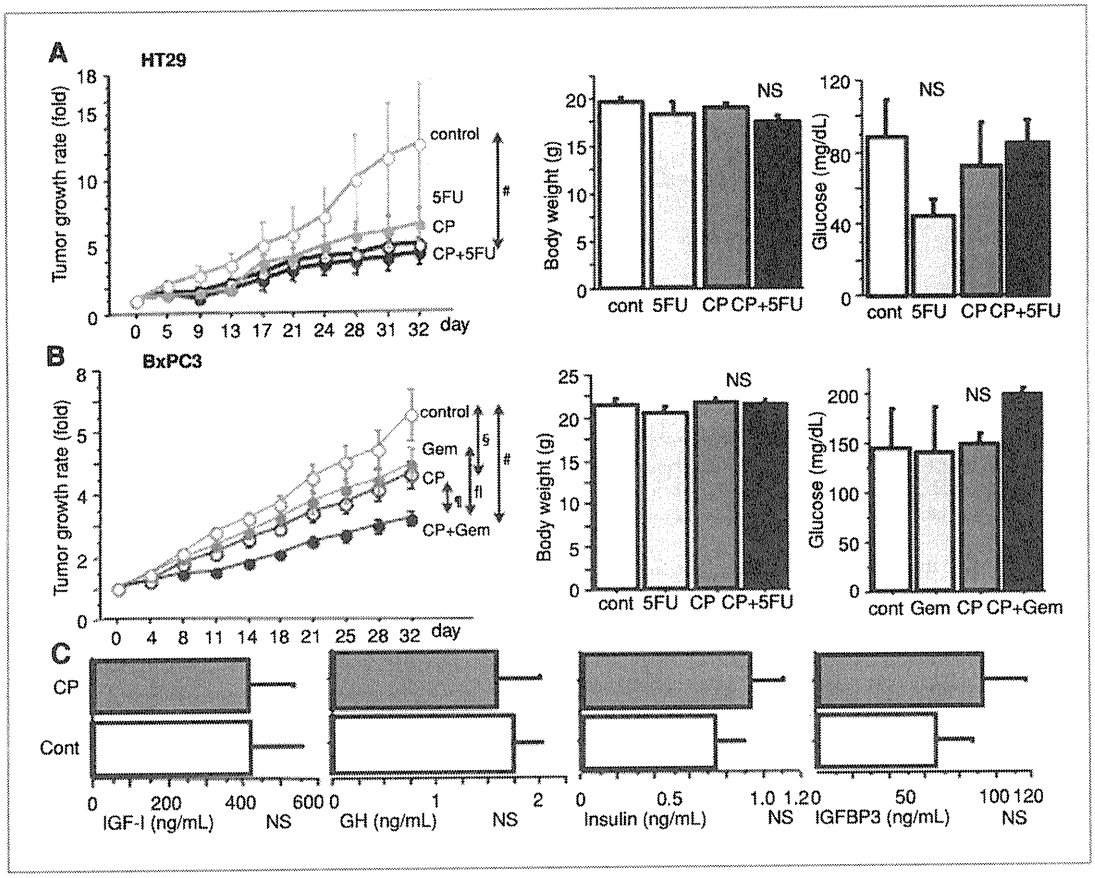

Figure 3. The effect of figitumumab on established tumor on mice. A, 125 μg CP-751,871 (twice a week, i.p.) tended to reduce relative size of s.c. tumors of HT29 on nude mice. The combination of CP-751,871 and 5-FU (once a week, i.p.) suppressed tumor growth (#, $P = 0.0268$ compared to control, each group $n = 8$). There are no significant differences between each single therapy and the combination. There are not significant differences in both body weight and blood glucose level on sacrifice (B) CP-751,871 alone reduced relative size of BxPC3 tumors on nude mice (§, $P = 0.0133$ compared to control, each group $n = 8$). The combination with CP-751,871 and gemcitabine blocked tumor growth most (#, $P < 0.0001$ compared to control). The effects of combination were more than the monotherapies (¶, $P = 0.0274$ compared to mAb; fl, $P = 0.0036$ to gemcitabine). Both body weight and blood glucose level on sacrifice were not different among 4 groups. C, ELISA showed that CP-751,871 did not affect blood concentrations of IGF-I (mean ± SE in mice treated with CP-751,871 was 415 ng/mL ± 122 and that in mice treated with control was 420 ng/mL ± 137, $P = 0.9775$), growth hormone (1.58 ng/mL ± 0.42 and 1.74 ng/mL ± 0.27, respectively, $P = 0.7470$), insulin (0.92 ng/mL ± 0.19 and 0.73 ng/mL ± 0.16, respectively, $P = 0.4446$), and IGF binding protein-3 (92. 07 ng/mL ± 24.92 and 66.45 ng/mL ± 20.97, respectively, $P = 0.4446$) on sacrifice.

Published OnlineFirst June 3, 2011; DOI:10.1158/1078-0432.CCR-10-3131

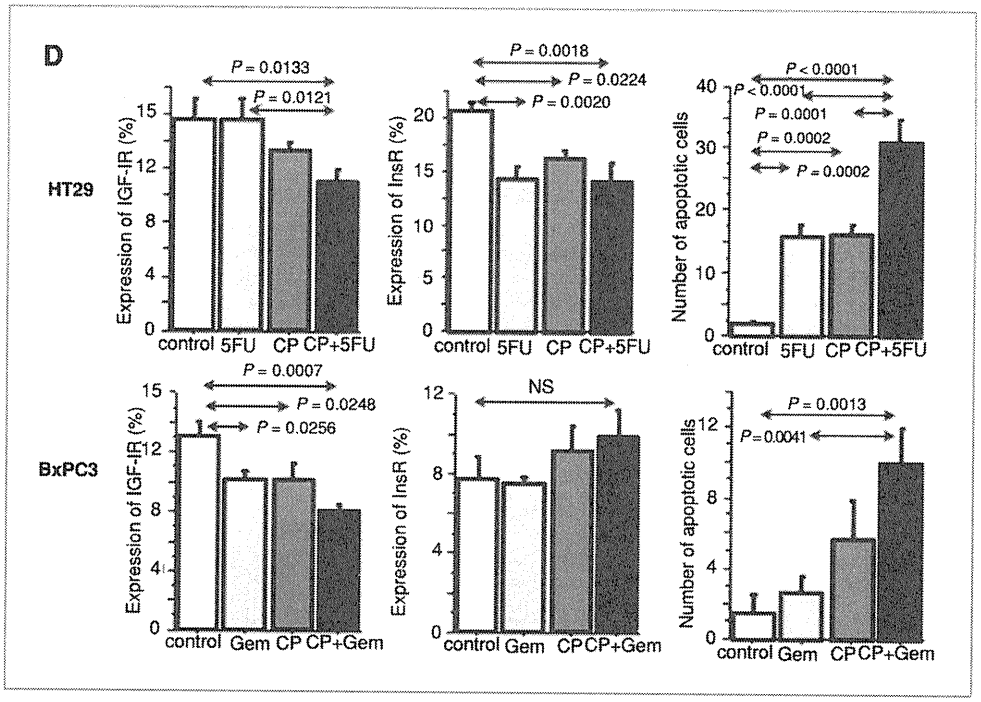

Figure 3. (*Continued*) D, receptors expressions and apoptosis induction in SC tumors on sacrifice were assessed by immunostaining. CP-751,871 alone reduced the expression of IGF-IR in BxPC3 tumors but not in HT29. Combination treatments reduce both expression of IGF-IR in both cell types and InsR in HT29, but up-regulated InsR in BxPC3. TUNEL assay shows that CP-751, 871 induced apoptosis in HT29 and enhanced both gemcitabine and 5-FU induced apoptosis. *Post hoc t* test was by Fischer's PLSD. Cont, control; CP, CP-751,871 (figitumumab); Gem, gemcitabine.

xenografts, and the number of apoptotic cells was greatest in the combination group. In BxPC3 xenografts, figitumumab up-regulated gemcitabine-induced apoptosis, although each individual treatment did not induce apoptosis significantly.

The results indicate that figitumumab might be effective for GI cancers, HT29 and BxPC3; however, both cell lines have wild-type *k-ras* so we asked whether the same effects could be observed in *k-ras* mutant cell lines.

Blockade of signal transduction in *k-ras* mutated cells

It has been reported that *k-ras* mutation is one of key genetic events in GI malignancies, and is associated with significant resistance to molecular targeted therapies such as cetuximab (44). There is therefore a dearth of novel and effective therapies in this subset of tumors. To assess the effect of figitumumab on the IGF/receptor axis in GI cancers with *k-ras* mutation, we examined 3 GI cancer cell lines, DLD-1, MIAPaca2, and TE-1 with this mutation. One μg/mL figitumumab blocked autophosphorylation of IGF-IR from 1 to 48 hours in all 3 cell lines (Fig. 4A). Downstream signals of Akt-1 and the ERKs were also blocked by 1 μg/mL figitumumab. Although the effect of this mAb on the ERKs showed dose dependency in all 3 cell lines, a low dose of 0.1 μg/mL figitumumab blocked Akt effectively (Fig. 4B). These data show that figitumumab can block IGF-I signals in GI cancers with *k-ras* mutations.

In addition to IGF-I, 1 μg/mL figitumumab blocked IGF-II induced both phosphorylation of Akt and ERKs in DLD-1 (Fig. 4C). The results indicate that this mAb can block IGF signals effectively for GI malignancies having a mutation in *k-ras*.

The effect of this antibody on insulin signaling was limited. High doses of 10 μg/mL figitumumab could block insulin-induced autophosphorylation of InsR and activation of Akt-1, but not that of ERKs in DLD1 (Fig. 4D). One μg/mL figitumumab did not inhibit insulin signals between 30 minutes and 48 hours exposures in DLD1.

The *in vitro* effect on cell growth and survival for *k-ras* mutated cells

Next, we assessed the effect of this drug on the *in vitro* growth and survival of *k-ras* mutated GI cancers. Colony formation assays showed that this mAb reduced the *in vitro* tumorigenicity of both DLD1 and MIAPaca2 in a dose-dependent fashion (Fig. 5A). One μg/mL figitumumab also effectively reduced colony formation of TE1.

Caspase-3 assays revealed that this antibody enhanced 5-FU induced apoptosis synergistically in DLD1 and additively in the other cell lines, MIAPaca2 and TE1 (Fig. 5B).

Published OnlineFirst June 3, 2011; DOI:10.1158/1078-0432.CCR-10-3131

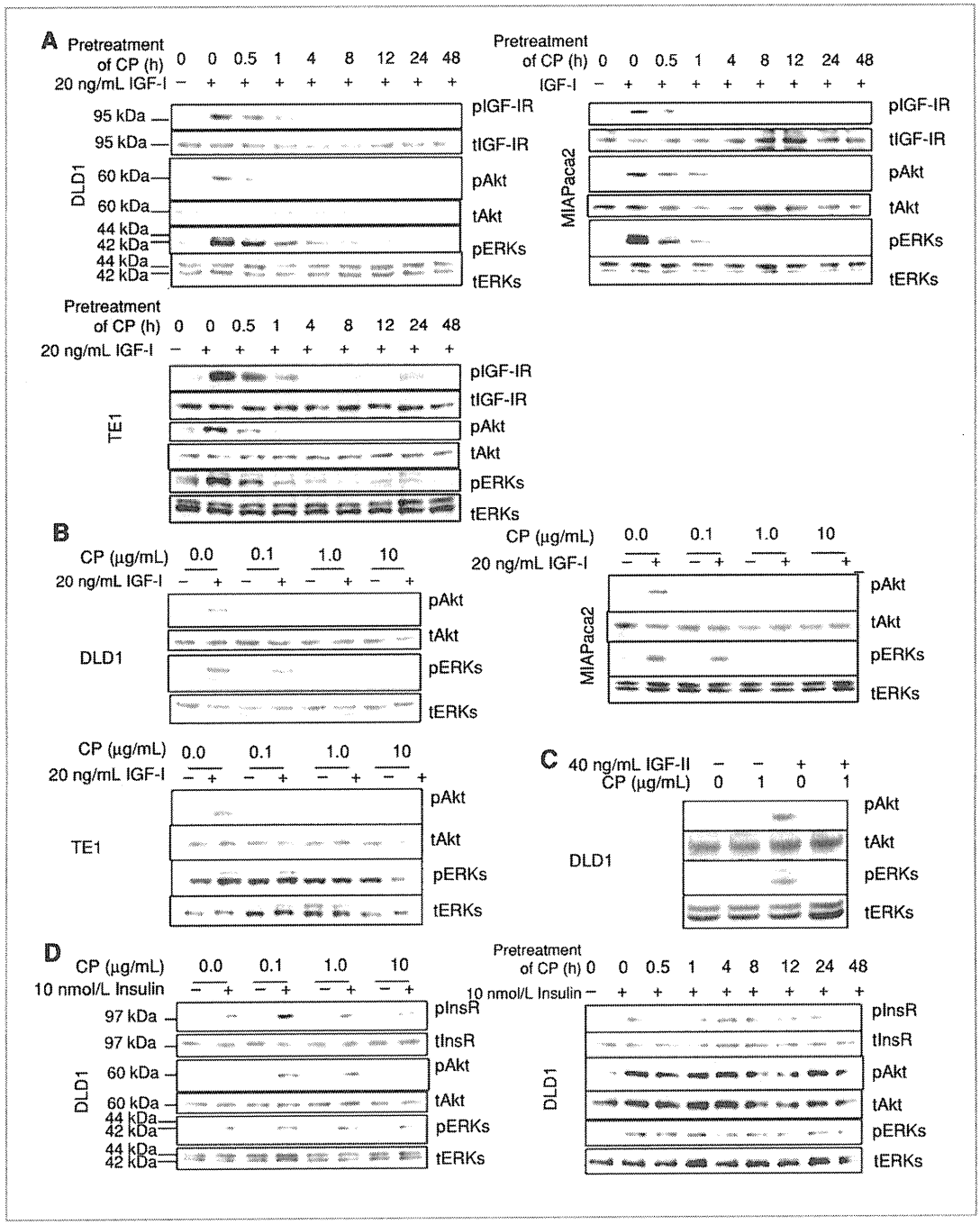

Figure 4. The effect of signal transduction on gastrointestinal cancer cells with *k-ras* mutation. A, with incubation with 1 μg/mL figitumumab from 1 to 48 hours, this mAb effectively blocked IGF-I–stimulated autophosphorylation of IGF-IR and both activation of Akt and ERKs in 3 cell lines; colorectal adenocarcinoma, DLD-1; pancreatic adenocarcinoma, MIAPaca2; and esophageal squamous cell carcinoma, TE1. B, ligand induced phospholyration of down-stream, Akt and ERKs, was blocked by 3 hours treatment with figitumumab, the former tend to be seen in lower dose of figitumumab than the latter. C, in DLD-1, this mAb blocked IGF-II stimulated both phosphorylation of Akt and ERKs. D, to block 10 nmol/L insulin-induced signal transduction, more than 10 μg/mL figitumumab (3 hours incubation) are needed in DLD-1.

Published OnlineFirst June 3, 2011; DOI:10.1158/1078-0432.CCR-10-3131

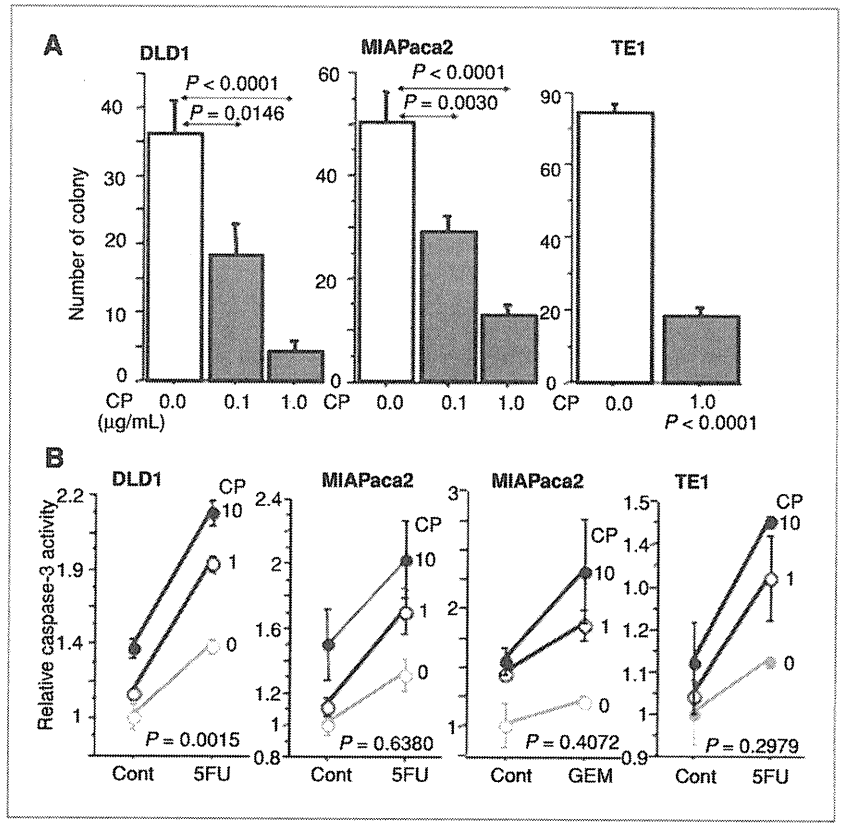

Figure 5. The effect of figitumumab on colony formation and survival in *k-ras* mutated GI cancer cells. A, the mAb reduced colony formation with dose dependency in both DLD-1 and MIAPaca2. One μg/mL figitumumab effectively blocked colony formation in TE1. B, caspase-3 assay shows that CP-781871 enhanced chemotherapy induced apoptosis; synergistically with 5-FU in DLD-1, and additively with gemcitabine in MIAPaca2 and with 5-FU in MIAPaca2 and TE1.

This drug strengthened the effect of gemcitabine additively in MIAPaca2. These results suggest that figitumumab has significant antitumor effects on GI cancer cells with *k-ras* mutations.

Figitumumab suppressed *k-ras* mutated tumors in mice

To assess the *in vivo* effect of this drug on GI cancers with *k-ras* mutations, DLD1 cells were inoculated s.c. in nude mice and allowed to form evident tumors. DLD1 tumor-bearing mice were treated with an i.p. injection of 125 μg figitumumab (twice a week) or control. This mAb suppressed tumor growth significantly (Fig. 6A). Then, the combination effect of this antibody and 5-FU was assessed. This combination suppressed tumor growth more effectively than monotherapy, however these additive effects were limited. None of these treatments affected murine body weight on sacrifice.

The *in vivo* effect of figitumumab on another *k-ras* mutated cell line, MIAPaca2, was then assessed. This drug inhibited dramatically tumor growth of MIAPaca2 xenografts (Fig. 6B). Both monotherapies of figitumumab and gemcitabine clearly reduced tumor growth ($P = 0.0036$ and 0.0012 compared to control, respectively), however the combination inhibited growth more effectively ($P < 0.0001$). Although treatment with gemcitabine was associated with reduced murine weight on sacrifice, the mAb alone did not affect animal weight. Figitumumab increased serum glucose concentrations on sacrifice more than gemcitabine monotherapy.

To assess the effect of treatments on both cell proliferation and apoptosis, resected tumor tissues were analyzed (Fig. 6C). In DLD1 tumors, only the combination therapy effectively reduced cell proliferation. In MIAPaca2 tumors, gemcitabine down-regulated proliferation, which was enhanced by figitumumab. In DLD1 tumors, 5-FU induced apoptosis and this antibody increased this effect. In MIAPaca2 tumors, gemcitabine induced apoptosis and this mAb up-regulated this effect. These results suggest that the antitumor effects of figitumumab are observed even in the presence of *k-ras* mutation in GI cancers.

Discussion

GI carcinomas are composed of a variety of histological types, and patients with these cancers show vastly different clinical courses. GI cancers are often diagnosed in advanced stages having lymph node/distant metastases and peritoneal dissemination, and in these cases there are extremely limited

Published OnlineFirst June 3, 2011; DOI:10.1158/1078-0432.CCR-10-3131

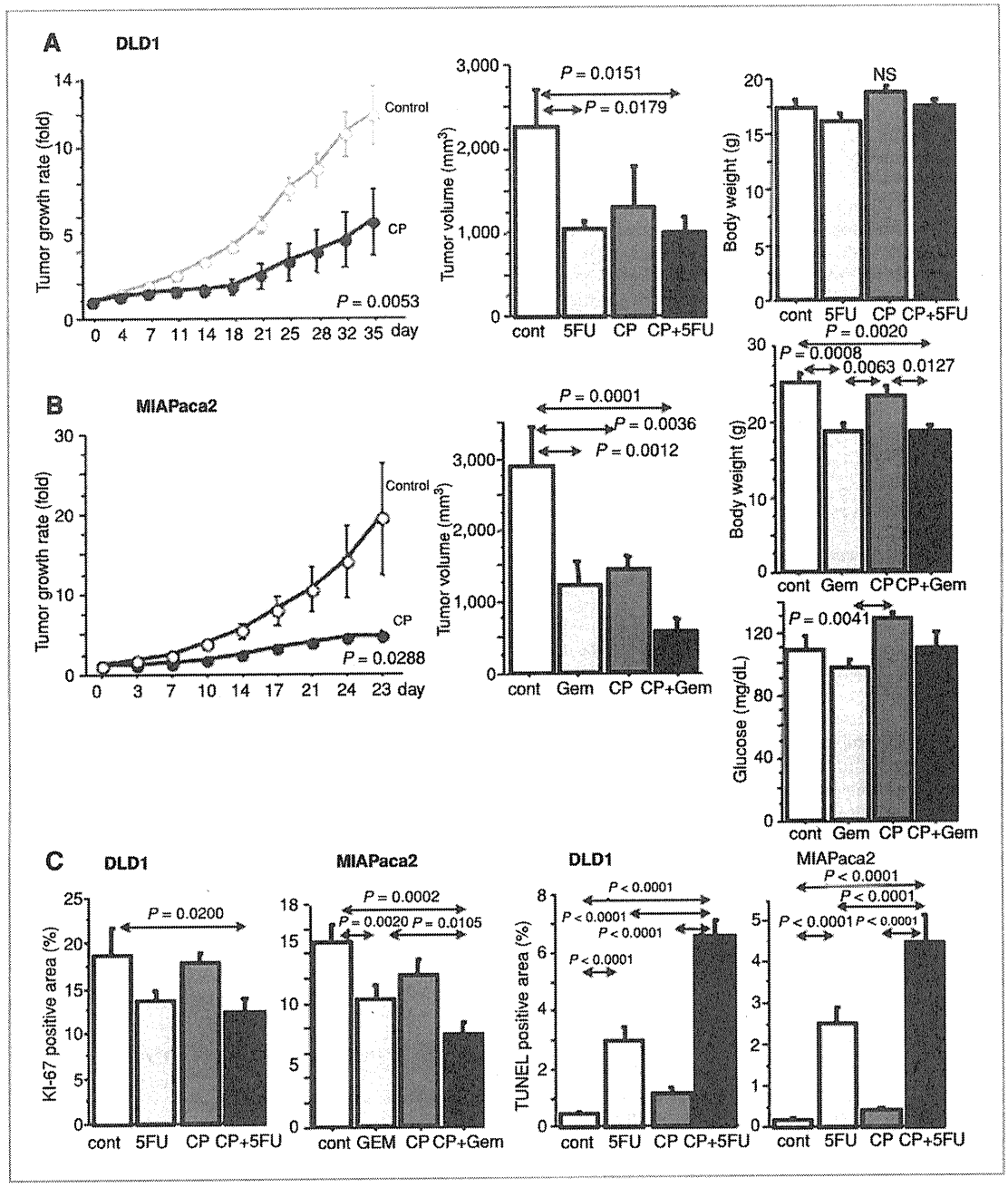

Figure 6. The effects of figitumumab on *k-ras* mutated GI cancer on mice. A, figitumumab suppressed tumor growth rate of DLD-1 on mice ($n = 8$, $P = 0.0053$). Tumor volume of mice treated with combination of this mAb and 5-FU showed least of all groups ($P = 0.0151$, the combination vs. control, each group $n = 8$), however there are no significant differences between each monotherapy and the combination. Body weight of mice on sacrifice was not influenced by treatments. B, figitumumab inhibited tumor growth rate of MIAPaca2 on mice ($n = 8$, $P = 0.0288$). The combination of this antibody and gemcitabine suppressed tumor volume most effectively of all ($P < 0.0001$, the combination vs. control, each group $n = 8$), however there are no significant differences between each monotherapy and the combination. Gemcitabine decreased murine weight on sacrifice and figitumumab single therapy up-regulated blood glucose on sacrifice. C, the combination treatment reduced Ki-67 label in DLD1. Gemcitabine alone reduce tumor cell growth and figitumumab enhanced this effect. In both tumors, 5-FU induced TUNEL positive area and figitumumab strengthened this effect. *Post hoc t* test was by Fischer's PLSD. Cont, control; CP, CP-751,871 (figitumumab); Gem, gemcitabine.

Published OnlineFirst June 3, 2011; DOI:10.1158/1078-0432.CCR-10-3131

options. GI malignancies are thus higher in overall mortality rates compared to their incidence rates (1). IGF-mediated growth-responsiveness is found in most GI cancer cells, including esophagus, intestine, pancreas, and liver (12, 15, 16, 19). High expression of both IGF-IR and the ligands in tumor tissues has indicated continuous activation of this system by paracrine and autocrine loops (19, 45). The expression of IGF-IR/IGF-II might be useful for the predictive marker of recurrence and poor prognosis in ESCC (15). The functional significance of IGF-IR has been showed as cancer growth inhibition by anti–IGF-IR antibodies (19, 32). Here, we used a new IGF-IR mAb, figitumumab, for the accurate dissection of the responsible signaling pathways. The results indicate that this strategy is promising for the treatment of GI tumors, not only as a monotherapy but especially in combination with cytotoxic drugs. We first showed that figitumumab enhanced the effects of both 5-FU and gemcitabine. Resistance to chemotherapy is a serious problem in patients with GI malignancies and this approach has the potential for overcoming this difficulty. It is important to note that our studies show that figitumumab is effective against a wide range of GI carcinomas, and these effects are not unique to 1 or 2 unusual cell lines.

Cetuximab is a powerful molecular targeted drug for patients with colorectal cancer, however, it shows limited or no efficacy for *k-ras* mutated cancers(43, 44). Although IGF-IR might be the next important target in human GI carcinomas, there is no information about IGF-IR–targeted therapy in *k-ras* mutated cancers. In this study, figitumumab showed antitumor effects for *k-ras* mutated cancers as well as wild-type ones both *in vitro* and *in vivo*. Our previous data in GI carcinomas indicated that IGF-IR blockade inhibited Akt signals more than ERK signaling, so the PI3-K/Akt pathway might play a more important role than the ras/MAPK pathway in the downstream signals of the IGF/IGF-IR axis (15, 35–37). This could explain why figitumumab is active for *k-ras* mutated GI cancer cells, however further studies are needed to analyze this mechanism precisely. Although we did not assess the efficacy of this drug for patients with GI cancers with and without *k-ras* mutations, these data might support the use of this mAb in this clinical setting. Further studies will be needed to clarify this hypothesis.

A major obstacle to the targeting of IGF-IR is the close homology of the IGF-IR and the IR kinase domains (46). Therefore, it is important that any strategy designed to block IGF signaling has specificity for IGF-IR and without a detrimental influence on IR signals. We show here that figitumumab does not suppress insulin-induced InsR- or Akt-phosphorylation in DLD1 indicating a high degree of receptor selectivity at tumor-active doses with this molecular-targeted therapy. Plasma concentrations of glucose, IGF-I, insulin, growth hormone, IGFBP3 were not influenced by this mAb. Moreover, body weight was monitored and not significantly affected by this therapy. This lack of effect on the insulin pathway and clinical toxicity leads us to believe that these combinations will have minimal adverse effects in clinical applications.

As figitumumab is of the IgG2 subtype, which is usually a poor activator of cellular immune responses, ongoing clinical trials may clarify whether this agent has significantly different properties from the IgG1 class from which class most other mAbs targeting IGF-IR are derived. According to several clinical studies, the main adverse effects of IGF-IR mAb are hyperglycemia, mild skin toxicities, and fatigue (41, 47, 48). IGF-IR mAb has been reported to cause hyperglycemia in about 20% of patients but this has generally been tolerable, mild to moderate, reversible, and manageable with usual oral hypoglycemic drugs. Patients with previous glucose intolerance or with steroids usage might be at increased risk of hyperglycemia.

It is also important to define surrogate markers of response for modern targeted agents. Although we could not assess this completely in these murine models, several possibilities have been put forward. One is that circulating tumor cells would be a marker, as treatment with figitumumab decreased both total circulating tumor cell count and IGF-IR–positive circulating tumor cell count (41). Another is that high concentration of serum-free IGF-I may be a marker of high responder of patients with non small cell lung carcinoma treated with figitumumab.

Recently, a new role of the IGF-IR has been identified that there is significant cross-talk between the IGF-IR and other tyrosine kinase receptors. For example, many patients with breast cancer who achieve an initial response to trastuzumab acquire secondary resistance. One mechanism of resistance has been showed to be overexpression of IGF-IR (49) and another is the formation of IGF-IR/Her2 heterodimers (50). These data suggest that IGF-IR blockade may be specifically effective for breast cancer patients with trastuzumab-resistant tumors.

Thus, in this study, we show that figitumumab suppresses the tumorigenicity and survival of GI cancers with or without *k-ras* mutations, by blocking Akt and ERK activation, both *in vitro* and in animal models. It also enhances chemotherapy efficacy without significantly influencing InsR signals at therapeutically effective doses. This study thus validates IGF-IR as a therapeutic target in GI carcinomas and suggest that figitumumab may be a promising antitumor therapeutic for these diseases.

Disclosure of Potential Conflicts of Interest

No potential conflicts of interest were disclosed.

Grant Support

This work was supported by grants-in-aid from the Ministry of Education, Culture, Sports, Science, and Technology and from the Ministry of Health, Labour and Welfare, Japan.

The costs of publication of this article were defrayed in part by the payment of page charges. This article must therefore be hereby marked *advertisement* in accordance with 18 U.S.C. Section 1734 solely to indicate this fact.

Received November 23, 2010; revised May 19, 2011; accepted May 24, 2011; published OnlineFirst June 3, 2011.

Published OnlineFirst June 3, 2011; DOI:10.1158/1078-0432.CCR-10-3131

References

1. American Cancer Society. Cancer Facts & Figures 2010. Available from: http://wwwcancerorg/acs/groups/content/@epidemiologysurveilance/documents/document/acspc-026238pdf2010.
2. Baserga R. Oncogenes and the strategy of growth factors. Cell 1994;79:927–30.
3. Adachi Y, Yamamoto H, Imsumran A, et al. Insulin-like growth factor-I receptor as a candidate for a novel molecular target in the gastrointestinal cancers. Dig Endosc 2006;18:245–51.
4. Miller BS, Yee D. Type I insulin-like growth factor receptor as a therapeutic target in cancer. Cancer Res 2005;65:10123–7.
5. Ullrich A, Gray A, Tam AW, Yang-Feng T, Tsubokawa M, Collins C, et al. Insulin-like growth factor I receptor primary structure: comparison with insulin receptor suggests structural determinants that define functional specificity. Embo J 1986;5:2503–12.
6. Baselga J, Norton L, Albanell J, Kim YM, Mendelsohn J. Recombinant humanized anti-HER2 antibody (Herceptin) enhances the antitumor activity of paclitaxel and doxorubicin against HER2/neu overexpressing human breast cancer xenografts. Cancer Res 1998;58:2825–31.
7. Yu H, Rohan T. Role of the insulin-like growth factor family in cancer development and progression. J Natl Cancer Inst 2000;92:1472–89.
8. Sara VR, Hall K. Insulin-like growth factors and their binding proteins. Physiol Rev 1990;70:591–614.
9. Remacle-Bonnet M, Garrouste F, el Atiq F, Roccabianca M, Marvaldi J, Pommier G. des-(1–3)-IGF-I, an insulin-like growth factor analog used to mimic a potential IGF-II autocrine loop, promotes the differentiation of human colon-carcinoma cells. Int J Cancer 1992;52:910–7.
10. Ma J, Pollak MN, Giovannucci E, Chan JM, Tao Y, Hennekens CH, et al. Prospective study of colorectal cancer risk in men and plasma levels of insulin-like growth factor (IGF)-I and IGF-binding protein-3. J Natl Cancer Inst 1999;91:620–5.
11. Harper J, Burns JL, Foulstone EJ, Pignatelli M, Zaina S, Hassan AB. Soluble IGF2 receptor rescues Apc(Min/+) intestinal adenoma progression induced by Igf2 loss of imprinting. Cancer Res 2006;66:1940–8.
12. Lahm H, Suardet L, Laurent PL, Fischer JR, Ceyhan A, Givel JC, et al. Growth regulation and co-stimulation of human colorectal cancer cell lines by insulin-like growth factor I, II and transforming growth factor alpha. Br J Cancer 1992;65:341–6.
13. Thompson MA, Cox AJ, Whitehead RH, Jonas HA. Autocrine regulation of human tumor cell proliferation by insulin-like growth factor II: an in-vitro model. Endocrinology 1990;126:3033–42.
14. Chen SC, Chou CK, Wong FH, Chang CM, Hu CP. Overexpression of epidermal growth factor and insulin-like growth factor-I receptors and autocrine stimulation in human esophageal carcinoma cells. Cancer Res 1991;51:1898–903.
15. Imsumran A, Adachi Y, Yamamoto H, Li R, Wang Y, Min Y, et al. Insulin-like growth factor-I receptor as a marker for prognosis and a therapeutic target in human esophageal squamous cell carcinoma. Carcinogenesis 2007;28:947–56.
16. Caro JF, Poulos J, Ittoop O, Pories WJ, Flickinger EG, Sinha MK. Insulin-like growth factor I binding in hepatocytes from human liver, human hepatoma, and normal, regenerating, and fetal rat liver. J Clin Invest 1988;81:976–81.
17. Verspohl EJ, Maddux BA, Goldfine ID. Insulin and insulin-like growth factor I regulate the same biological functions in HEP-G2 cells via their own specific receptors. J Clin Endocrinol Metab 1988;67:169–74.
18. Kim SO, Park JG, Lee YI. Increased expression of the insulin-like growth factor I (IGF-I) receptor gene in hepatocellular carcinoma cell lines: implications of IGF-I receptor gene activation by hepatitis B virus X gene product. Cancer Res 1996;56:3831–6.
19. Bergmann U, Funatomi H, Yokoyama M, Beger HG, Korc M. Insulin-like growth factor I overexpression in human pancreatic cancer: evidence for autocrine and paracrine roles. Cancer Res 1995;55:2007–11.
20. Ajisaka H, Fushida S, Yonemura Y, Miwa K. Expression of insulin-like growth factor-2, c-MET, matrix metalloproteinase-7 and MUC-1 in primary lesions and lymph node metastatic lesions of gastric cancer. Hepatogastroenterology 2001;48:1788–92.
21. Levitt RJ, Pollak M. Insulin-like growth factor-I antagonizes the antiproliferative effects of cyclooxygenase-2 inhibitors on BxPC-3 pancreatic cancer cells. Cancer Res 2002;62:7372–6.
22. Baserga R. The insulin-like growth factor I receptor: a key to tumor growth? Cancer Res 1995;55:249–52.
23. Sell C, Rubini M, Rubin R, Liu JP, Efstratiadis A, Baserga R. Simian virus 40 large tumor antigen is unable to transform mouse embryonic fibroblasts lacking type 1 insulin-like growth factor receptor. Proc Natl Acad Sci U S A 1993;90:11217–21.
24. Simmons JG, Pucilowska JB, Lund PK. Autocrine and paracrine actions of intestinal fibroblast-derived insulin-like growth factors. Am J Physiol 1999;276:G817–27.
25. Nosho K, Yamamoto H, Taniguchi H, Adachi Y, Yoshida Y, Arimura Y, et al. Interplay of insulin-like growth factor-II, insulin-like growth factor-I, insulin-like growth factor-I receptor, COX-2, and matrix metalloproteinase-7, play key roles in the early stage of colorectal carcinogenesis. Clin Cancer Res 2004;10:7950–7.
26. Nosho K, Yamamoto H, Adachi Y, Endo T, Hinoda Y, Imai K. Gene expression profiling of colorectal adenomas and early invasive carcinomas by cDNA array analysis. Br J Cancer 2005;92:1193–200.
27. Nakamura M, Miyamoto S, Maeda H, Ishii G, Hasebe T, Chiba T, et al. Matrix metalloproteinase-7 degrades all insulin-like growth factor binding proteins and facilitates insulin-like growth factor bioavailability. Biochem Biophys Res Commun 2005;333:1011–6.
28. Miyamoto S, Nakamura M, Yano K, Ishii G, Hasebe T, Endoh Y, et al. Matrix metalloproteinase-7 triggers the matricrine action of insulin-like growth factor-II via proteinase activity on insulin-like growth factor binding protein 2 in the extracellular matrix. Cancer Sci 2007;98:685–91.
29. Adachi Y, Li R, Yamamoto H, Min Y, Piao W, Wang Y, et al. Insulin-like growth factor-I receptor blockade reduces the invasiveness of gastrointestinal cancers via blocking production of matrilysin. Carcinogenesis 2009;30:1305–13.
30. Pandini G, Frasca F, Mineo R, Sciacca L, Vigneri R, Belfiore A. Insulin/insulin-like growth factor I hybrid receptors have different biological characteristics depending on the insulin receptor isoform involved. J Biol Chem 2002;277:39684–95.
31. Schoen RE, Weissfeld JL, Kuller LH, Thaete FL, Evans RW, Hayes RB, et al. Insulin-like growth factor-I and insulin are associated with the presence and advancement of adenomatous polyps. Gastroenterology 2005;129:464–75.
32. Cohen BD, Baker DA, Soderstrom C, Tkalcevic G, Rossi AM, Miller PE, et al. Combination therapy enhances the inhibition of tumor growth with the fully human anti-type 1 insulin-like growth factor receptor monoclonal antibody CP-751,871. Clin Cancer Res 2005;11:2063–73.
33. Wang Y, Hailey J, Williams D, Wang Y, Lipari P, Malkowski M, et al. Inhibition of insulin-like growth factor-I receptor (IGF-IR) signaling and tumor cell growth by a fully human neutralizing anti-IGF-IR antibody. Mol Cancer Ther 2005;4:1214–21.
34. Wittman M, Carboni J, Attar R, Balasubramanian B, Balimane P, Brassil P, et al. Discovery of a (1H-benzoimidazol-2-yl)-1H-pyridin-2-one (BMS-536924) inhibitor of insulin-like growth factor I receptor kinase with *in vivo* antitumor activity. J Med Chem 2005;48:5639–43.
35. Adachi Y, Lee CT, Coffee K, Yamagata N, Ohm JE, Park KH, et al. Effects of genetic blockade of the insulin-like growth factor receptor in human colon cancer cell lines. Gastroenterology 2002;123:1191–204.
36. Min Y, Adachi Y, Yamamoto H, Ito H, Itoh F, Lee CT, et al. Genetic blockade of the insulin-like growth factor-i receptor: a promising strategy for human pancreatic cancer. Cancer Res 2003;63:6432–41.
37. Min Y, Adachi Y, Yamamoto H, Imsumran A, Arimura Y, Endo T, et al. Insulin-like growth factor I receptor blockade enhances chemotherapy and radiation responses and inhibits tumour growth in human gastric cancer xenografts. Gut 2005;54:591–600.
38. Haluska P, Shaw HM, Batzel GN, Yin D, Molina JR, Molife LR, et al. Phase I dose escalation study of the anti insulin-like growth factor-I receptor monoclonal antibody CP-751,871 in patients with refractory solid tumors. Clin Cancer Res 2007;13:5834–40.
39. Lacy MQ, Alsina M, Fonseca R, Paccagnella ML, Melvin CL, Yin D, et al. Phase I, pharmacokinetic and pharmacodynamic study of the

Published OnlineFirst June 3, 2011; DOI:10.1158/1078-0432.CCR-10-3131

anti-insulin-like growth factor type 1 Receptor monoclonal antibody CP-751,871 in patients with multiple myeloma. J Clin Oncol 2008;26:3196–203.

40. Karp DD, Paz-Ares LG, Novello S, Haluska P, Garland L, Cardenal F, et al. Phase II study of the anti-insulin-like growth factor type 1 receptor antibody CP-751,871 in combination with paclitaxel and carboplatin in previously untreated, locally advanced, or metastatic non-small-cell lung cancer. J Clin Oncol 2009;27:2516–22.
41. de Bono JS, Attard G, Adjei A, Pollak MN, Fong PC, Haluska P, et al. Potential applications for circulating tumor cells expressing the insulin-like growth factor-I receptor. Clin Cancer Res 2007;13:3611–6.
42. Molife LR, Fong PC, Paccagnella L, Reid AH, Shaw HM, Vidal L, et al. The insulin-like growth factor-I receptor inhibitor figitumumab (CP-751,871) in combination with docetaxel in patients with advanced solid tumours: results of a phase Ib dose-escalation, open-label study. Br J Cancer 2010;103:332–9.
43. Karapetis CS, Khambata-Ford S, Jonker DJ, O'Callaghan CJ, Tu D, Tebbutt NC, et al. K-ras mutations and benefit from cetuximab in advanced colorectal cancer. N Engl J Med 2008;359:1757–65.
44. Jimeno A, Messersmith WA, Hirsch FR, Franklin WA, Eckhardt SG. KRAS mutations and sensitivity to epidermal growth factor receptor inhibitors in colorectal cancer: practical application of patient selection. J Clin Oncol 2009;27:1130–6.
45. Lahm H, Amstad P, Wyniger J, Yilmaz A, Fischer JR, Schreyer M, et al. Blockade of the insulin-like growth-factor-I receptor inhibits growth of human colorectal cancer cells: evidence of a functional IGF-II-mediated autocrine loop. Int J Cancer 1994;58:452–9.
46. Adams TE, Epa VC, Garrett TP, Ward CW. Structure and function of the type 1 insulin-like growth factor receptor. Cell Mol Life Sci 2000;57:1050–93.
47. Tolcher AW, Sarantopoulos J, Patnaik A, Papadopoulos K, Lin CC, Rodon J, et al. Phase I, pharmacokinetic, and pharmacodynamic study of AMG 479, a fully human monoclonal antibody to insulin-like growth factor receptor 1. J Clin Oncol 2009;27:? 5800–7.
48. Kurzrock R, Patnaik A, Aisner J, Warren T, Leong S, Benjamin R, et al. A phase I study of weekly R1507, a human monoclonal antibody insulin-like growth factor-I receptor antagonist, in patients with advanced solid tumors. Clin Cancer Res. 2010;16:2458–65.
49. Lu Y, Zi X, Zhao Y, Mascarenhas D, Pollak M. Insulin-like growth factor-I receptor signaling and resistance to trastuzumab (Herceptin). J Natl Cancer Inst 2001;93:1852–7.
50. Nahta R, Yuan LX, Zhang B, Kobayashi R, Esteva FJ. Insulin-like growth factor-I receptor/human epidermal growth factor receptor 2 heterodimerization contributes to trastuzumab resistance of breast cancer cells. Cancer Res 2005;65:11118–28.

THE JOURNAL OF IMMUNOLOGY

The Development of Colitogenic CD4$^+$ T Cells Is Regulated by IL-7 in Collaboration with NK Cell Function in a Murine Model of Colitis

Osamu Yamaji, Takashi Nagaishi, Teruji Totsuka, Michio Onizawa, Masahiro Suzuki, Naoto Tsuge, Atsuhiko Hasegawa, Ryuichi Okamoto, Kiichiro Tsuchiya, Tetsuya Nakamura, Hisashi Arase, Takanori Kanai and Mamoru Watanabe

J Immunol; Prepublished online 13 February 2012;
doi:10.4049/jimmunol.1100371
http://www.jimmunol.org/content/early/2012/02/12/jimmunol.1100371

The Journal of Immunology is published twice each month by The American Association of Immunologists, Inc., 9650 Rockville Pike, Bethesda, MD 20814-3994.

Print ISSN: 0022-1767 Online ISSN: 1550-6606.

Published February 13, 2012, doi:10.4049/jimmunol.1100371

The Development of Colitogenic CD4$^+$ T Cells Is Regulated by IL-7 in Collaboration with NK Cell Function in a Murine Model of Colitis

Osamu Yamaji,*,[1] Takashi Nagaishi,*,[1] Teruji Totsuka,* Michio Onizawa,* Masahiro Suzuki,* Naoto Tsuge,* Atsuhiko Hasegawa,† Ryuichi Okamoto,* Kiichiro Tsuchiya,* Tetsuya Nakamura,* Hisashi Arase,‡,§,¶ Takanori Kanai,‖ and Mamoru Watanabe*

We previously reported that IL-7$^{-/-}$RAG$^{-/-}$ mice receiving naive T cells failed to induce colitis. Such abrogation of colitis may be associated with not only incomplete T cell maintenance due to the lack of IL-7, but also with the induction of colitogenic CD4$^+$ T cell apoptosis at an early stage of colitis development. Moreover, NK cells may be associated with the suppression of pathogenic T cells in vivo, and they may induce apoptosis of CD4$^+$ T cells. To further investigate these roles of NK cells, RAG$^{-/-}$ and IL-7$^{-/-}$RAG$^{-/-}$ mice that had received naive T cells were depleted of NK cells using anti-asialo GM1 and anti-NK1.1 Abs. NK cell depletion at an early stage, but not at a later stage during colitogenic effector memory T cell (T_{EM}) development, resulted in exacerbated colitis in recipient mice even in the absence of IL-7. Increased CD44$^+$CD62L$^-$ T_{EM} and unique CD44$^-$CD62L$^-$ T cell subsets were observed in the T cell-reconstituted RAG$^{-/-}$ recipients when NK cells were depleted, although Fas, DR5, and IL-7R expressions in this subset differed from those in the CD44$^+$CD62L$^-$ T_{EM} subset. NK cell characteristics were the same in the presence or absence of IL-7 in vitro and in vivo. These results suggest that NK cells suppress colitis severity in T cell-reconstituted RAG$^{-/-}$ and IL-7$^{-/-}$RAG$^{-/-}$ recipient mice through targeting of colitogenic CD4$^+$CD44$^+$CD62L$^-$ T_{EM} and, possibly, of the newly observed CD4$^+$CD44$^-$CD62L$^-$ subset present at the early stage of T cell development. *The Journal of Immunology*, **2012, 188: 000–000.**

The pathogenesis of inflammatory bowel diseases (IBD), such as Crohn's disease and ulcerative colitis in humans, is known to be associated with dysregulated immune responses to luminal contents including Ags derived from commensal bacteria in gut. In patients with Crohn's disease, for example, excessive amounts of proinflammatory cytokines, such as IFN-γ, TNF, and IL-17 (1), are secreted predominantly by CD4$^+$ T cells infiltrating colonic tissues. The activities of these cells are thought to reflect the severity of IBD. Additionally, it is known that adoptive transfer of CD4$^+$ naive T cells into lymphopenic immune-deficient animals, such as SCID and RAG$^{-/-}$ mice, induces chronic inflammation in the colon and is considered an animal model of IBD (2, 3).

IL-7 is an important cytokine that is associated with the proliferation of immature B and T cells (4) as well as with homeostatic maintenance of peripheral T cells in vivo (5, 6). We have previously reported that IL-7 is secreted by intestinal epithelia, especially goblet cells (7), and that spontaneous colitis that is similar to IBD in humans is induced in transgenic mice overexpressing IL-7 (8). Additionally, we have shown that the IL-7R^{high}CD4$^+$ T cell subset is pathogenic (9) when the cells are transferred into RAG$^{-/-}$ mice (10, 11). Moreover, we have also shown that adoptive transfer of naive T cells in RAG and IL-7 double-deficient (IL-7$^{-/-}$RAG$^{-/-}$) mice fails to induce colitis (10). Therefore, IL-7 was initially considered to be essential for the induction of colitis. However, it is known that IL-7 is not required for the in vitro differentiation from naive T cells into Th1 or Th17 cells (12). It is also known that the spontaneous proliferation, which is dependent on Ag ligation to the CD3/TCR complex, can be observed even in the T cell-reconstituted IL-7$^{-/-}$RAG$^{-/-}$ re-

*Department of Gastroenterology and Hepatology, Graduate School of Medical Science, Tokyo Medical and Dental University, Tokyo 113-8519, Japan; †Department of Immunotherapeutics, Graduate School of Medical Science, Tokyo Medical and Dental University, Tokyo 113-8519, Japan; ‡Laboratory of Immunochemistry, World Premier International Research Center, Immunology Frontier Research Center, Osaka University, Osaka 565-0871, Japan; §Department of Immunochemistry, Research Institute for Microbial Diseases, Osaka University, Osaka 565-0871, Japan; ¶Japan Science and Technology, Core Research for Evolutional Science and Technology, Saitama 332-0012, Japan; and ‖Department of Gastroenterology, Keio University School of Medicine, Tokyo 160-8582, Japan

[1]O.Y. and T.N. contributed equally to this work.

Received for publication February 11, 2011. Accepted for publication January 10, 2012.

This work was supported in part by Grants-in-Aid for Scientific Research (to T. Nagaishi, T.T., R.O., K.T., T. Nakamura, T.K., and M.W.), for Scientific Research on Priority Areas (to M.W.), and for Exploratory Research and Creative Scientific Research (to M.W.) from the Japanese Ministry of Education, Culture, Sports, Science, and Technology; the Japanese Ministry of Health, Labor, and Welfare (to M.W.); the Japan Medical Association (to M.W.); the Terumo Life Science Foundation (to M.W.); the Ohyama Health Foundation (to M.W.); the Yakult Bio-Science Foundation (to T.K. and T.T.); the Research Fund of Mitsukoshi Health and Welfare Foundation (to M.W. and R.O.); the Japan Foundation for Applied Enzymology (to M.O.); the Japan Health Sciences Foundation (to M.O.); the Memorial Fund of Nihon University Medical Alumni Association (to T. Nagaishi); the Abbott Japan Allergy Research Award (to T. Nagaishi); the Foundation for Advancement of International Science (to T. Nagaishi); and the Takeda Science Foundation (to T. Nagaishi).

Address correspondence and reprint requests to Dr. Mamoru Watanabe and Dr. Takashi Nagaishi, Department of Gastroenterology and Hepatology, Graduate School of Medical Science, Tokyo Medical and Dental University, 1-5-45 Yushima, Bunkyo-ku, Tokyo 113-8519, Japan. E-mail addresses: mamoru.gast@tmd.ac.jp (M.W.) and tnagaishi.gast@tmd.ac.jp (T.N.)

The online version of this article contains supplemental material.

Abbreviations used in this article: ASGM1, asialo GM1; EAE, experimental autoimmune encephalomyelitis; IBD, inflammatory bowel disease; LP, lamina propria; LPL, lamina propria lymphocyte; PI, propidium iodide; SPL, spleen; T_{EM}, effector memory T cell; WT, wild-type.

www.jimmunol.org/cgi/doi/10.4049/jimmunol.1100371

cipient mice (13, 14). Additionally, our recent studies suggested that effector $CD4^+$ T cells were able to induce colitis even in IL-$7^{-/-}RAG^{-/-}$ mice that were parabiosed with colitic $RAG^{-/-}$ mice that had been injected with naive T cells 6 wk previously (15). Moreover, a deparabiosed IL-$7^{-/-}RAG^{-/-}$ mouse, which was surgically separated from T cell-receiving $RAG^{-/-}$–IL-$7^{-/-}$ $RAG^{-/-}$ parabionts 6 wk after the initial surgery, still maintained chronic colitis for at least another 12 wk (16). These results suggested that the abrogation of colitis in the T cell-reconstituted IL-$7^{-/-}RAG^{-/-}$ mice may be associated with not only incomplete T cell maintenance due to the lack of IL-7, but also with another mechanism by which the colitogenic $CD4^+$ T cell development is suppressed.

It is known that NK cells are responsible for innate immune responses, including the depletion of tumor cells or cells infected with various kinds of viruses (17). Additionally, NK cells induce inflammation in tissues by the production of proinflammatory cytokines such as IFN-γ (18, 19). On the other hand, NK cells are also known to be critical for anti-inflammatory effects in the context of autoimmune diseases (20, 21). It has been reported that NK cells abrogate disease severity of experimental autoimmune encephalomyelitis (EAE) due to the suppression of pathogenic T cells (22, 23). It has also been reported that depletion of NK cells results in enhanced severity of a chronic colitis model (24). However, the mechanisms by which NK cells regulate inflammation in this colitis model have not been well described. In this regard, we hypothesized that the abrogation of colitogenic T cell development that we observed in naive T cell-receiving IL-$7^{-/-}$ $RAG^{-/-}$ mice is associated with the effect of NK cells. We therefore focused our analysis of this phenomenon on NK cells.

Materials and Methods

Animals

Wild-type (WT) C57BL/6 mice were purchased from Japan CLEA (Tokyo, Japan). Rag-deficient ($RAG^{-/-}$) mice on a C57BL/6 background were obtained from Taconic (Hudson, NY) and the Central Laboratories for Experimental Animals (Kanagawa, Japan). IL-$7^{-/-}$ mice were provided by Dr. R. Zamoyska (National Institute for Medical Research, London, U.K.) and were intercrossed with $RAG^{-/-}$ to generate IL-$7^{-/-}RAG^{-/-}$ mice. Mice were maintained under specific pathogen-free conditions in the Animal Care Facility of Tokyo Medical and Dental University. Donors and recipients were used between 8 and 16 wk age. All animal experimentations were approved by the Animal Review Board of Tokyo Medical and Dental University and were performed in accordance with institutional guidelines.

Abs

The following mAbs and reagents were obtained from BD Pharmingen (San Jose, CA): anti-CD3ε (145-2C11), anti-CD4 (RM4-5), anti-CD11b (M1/70), anti-CD11c (HL3), anti-CD27 (LG.3A10), anti-CD28 (37.51), anti-CD43 (S7), anti-CD44 (IM7), anti-CD45RB (16A), anti-CD51 (RMV-7), anti-CD62L (MEL-14), anti-CD69 (H1.2F3), anti-CD94 (18d3), anti-CD95, anti-CD178 (MFL4), anti-CD244.2 (2B4 B6 alloantigen), anti-Ly49C,I (5E6), anti-Ly49D (4E5), anti-Ly49F (HBF-719), anti-Ly49G2 (4D11), anti–IL-7Rα (A7R34), anti-NK1.1 (PK136), and streptavidin. Biotin-conjugated anti-mouse NKG2A/C/E, biotin-conjugated anti-mouse IL-7Rα (A7R34), FITC-conjugated anti-mouse pan-NK cells (CD49b), and FITC-conjugated anti-mouse CD3ε (145-2C11) mAbs were purchased from eBioscience (San Diego, CA).

Flow cytometry (FACS)

To detect the cell surface expression of a variety of molecules, isolated mononuclear cells from individual organs including spleen (SPL), mesenteric lymph node (MLN), and colonic lamina propria (LP) were analyzed by FACS using standard staining methods. Briefly, the cells were suspended in PBS containing 2% FBS, which was used as the suspension fluid for subsequent staining, preincubated with an FcγR-blocking mAb (anti-CD16/32; 2.4G2; BD Biosciences) for 15 min to prevent nonspecific binding by the secondary Ab, and washed with suspension fluid followed by staining with specific FITC-, PE-, PerCP-, allophycocyanin-, or biotin-labeled Abs for 20 min on ice. Standard two-, three-, or four-color flow cytometric analyses were performed using the FACSCalibur (Becton Dickinson, Sunnyvale, CA) with appropriate software (CellQuest; BD Biosciences). Background fluorescence was also assessed by staining with control irrelevant isotype-matched mAbs.

NK cell depletion in vivo

The anti-asialo GM1 (ASGM1) polyclonal Ab was obtained from Wako Chemicals (Osaka, Japan) and reconstituted according to the manufacturer's specifications. The anti-NK1.1 mAb was affinity purified from the culture supernatant of a hybridoma clone, PK136, obtained from the American Type Culture Collection (Manassas, VA). For effective depletion of NK cells in vivo, either the anti-ASGM1 polyclonal Ab (0.25 mg/mouse) or anti-NK1.1 mAb (0.5 mg/mouse) was injected i.p. into mice (25) at the indicated time points in each experiment. The same amount of rabbit Ig (Rockland Immunochemicals, Gilbertsville, PA) or mouse IgG2a (Medical & Biological Laboratories, Nagoya, Japan) were used as the controls, respectively, for some of experiments. Effective (~95%) depletion of NK cells in vivo was confirmed by FACS analysis of single cells derived from individual organs such as SPL, MLN, and colonic LP.

Purification of naive T cell subsets and induction of colitis

For naive T cell purification, splenic mononuclear cells were obtained from WT mice and $CD4^+$ T cells were isolated using anti-CD4 (L3T4) MACS magnetic beads (Miltenyi Biotec, Bergisch Gladbach, Germany) according to the manufacturer's instructions. Enriched $CD4^+$ T cells (94–97% pure as estimated by FACS) were then labeled with PerCP- or allophycocyanin-conjugated anti-CD4, PE- or allophycocyanin-conjugated anti-CD44, and FITC-conjugated anti-CD62L. Subpopulations of $CD4^+$ cells were generated by three-color sorting on a FACSAria (Becton Dickinson). All populations were 98.0% pure on reanalysis. To induce an animal model of chronic colitis, 5×10^5 $CD4^+CD44^-CD62L^+$ (naive) T cells were adoptively transferred i.p. into 8- to 12-wk-old $RAG^{-/-}$ or IL-$7^{-/-}RAG^{-/-}$ recipient mice as previously described (2, 3, 10).

Isolation of LP lymphocytes

LP lymphocytes (LPL) were isolated from healthy or colitic mice as previously described (10). Briefly, $RAG^{-/-}$ or IL-$7^{-/-}RAG^{-/-}$ recipient mice were sacrificed 6–12 wk after injection of naive T cells to induce colitis. The entire length of the colon was removed, opened longitudinally, washed with PBS, and cut into small pieces. The dissected tissues were incubated with Ca^{2+}-, Mg^{2+}-free HBSS containing 1 mM DTT (Sigma-Aldrich, St. Louis, MO) for 45 min to remove mucus, and the epithelial layer was then treated with 3.0 mg/ml collagenase (Roche Diagnostics, Mannheim, Germany) and 0.01% DNase (Worthington Biomedical, Freehold, NJ) for 2 h. The cells were pelleted, washed twice with PBS, and were then subjected to density gradient centrifugation using 40–75% isotonic Percoll (Amersham Biotech, Piscataway, NJ) solution diluted with HBSS. Isolated whole LP mononuclear cells were subjected to FACS to analyze each lymphocyte subset. In some experiments, such LP mononuclear cells were further labeled with allophycocyanin-conjugated anti-CD4 and FITC-conjugated anti-CD3 to isolate colitogenic $CD4^+$ T cell subsets by FACSAria. All populations were 98.0% pure on reanalysis. Isolated LP $CD4^+$ T cells were subjected to cytokine production and cytotoxicity assays.

Determination of clinical score of colitis

The clinical score of colitis was determined using previously described methods (26) with minor modifications and was assessed by trained individuals blinded to the treatment group. Briefly, initial body weight and wasting, hunching over, piloerection, diarrhea, and blood in the stool or per rectum of the T cell-receiving $RAG^{-/-}$ or IL-$7^{-/-}RAG^{-/-}$ recipient mice were assessed when sacrificed. For wasting, weight loss of <20% from baseline was assigned 0 points and weight loss of >20% was assigned 1 point. For hunched over appearance, no obvious hunching was assigned 0 point, and extensive hunching was assigned as 1 point. For colon thickening, normal features were assigned 0 points, mild thickening was assigned 1 point, moderate thickening was assigned 2 points, and severe thickening was assigned 3 points. For stool consistency, 0 points were assigned to well-formed pellets, 1 point to pasty and semiformed stools that did not adhere to the anus, and 2 points to liquid stools that did adhere to the anus. An additional point was added if gross blood was noted. The scores of these parameters were added, resulting in a total clinical score ranging from 0 (healthy) to 8 (maximal colitis activity).

Histopathological examination of colitis

Mice receiving naive T cells were sacrificed 6 or 12 wk after the T cell transfer, and colonic specimens taken from proximal, middle, and distal colons were subjected to histopathological assessment. For this assessment, tissue samples were fixed in 10% neutral-buffered formalin. Paraffin-embedded sections (5 μm) were stained with H&E. The H&E-stained sections were analyzed without prior knowledge of the type of donors, recipients, and treatments. The degree of inflammation in the colon was graded according to a modification of the previously described scoring system (26, 27). Briefly, for mucosal damage, 0 points were assigned to normal appearance, 1 point to discrete lymphoepithelial lesions, 2 points to diffuse crypt elongation, and 3 points to extensive crypt elongation or mucosal erosion/ulceration. For cell infiltration the points assigned were: 0, to normal, or presence of occasional leukocytes; 1, to widely scattered leukocytes or focal aggregates of leukocytes; 2, to confluence of leukocytes extending into the submucosa with focal effacement of the muscularis; 3, to transmural extension of leukocyte infiltration. For crypt abscess, the assigned points were: 0, to no crypt abscess; 1, to the presence of crypt abscess. The cumulative degree of these parameters was calculated as a total histological score ranging from 0 (no change) to 21 (extensive cell infiltration and tissue damage).

ELISA

To measure cytokine production, 1×10^5 LP $CD4^+$ T cells were cultured in 200 μl RPMI 1640 (Sigma-Aldrich) supplemented with 10% heat-inactivated FBS, 500 U/ml penicillin, 100 μg/ml streptomycin (Sigma-Aldrich), 10 mM HEPES, 1% nonessential amino acids, and 50 μM 2-ME (Life Technologies Invitrogen, Carlsbad, CA), termed complete RPMI 1640, in the presence of 5 μg/ml plate-bound anti-CD3ε (145-2C11) and 2 μg/ml soluble anti-CD28 (37.51) mAbs on flat-bottom 96-well plates (Costar, Cambridge, MA) at 37°C in a humidified atmosphere incubator containing 5% CO_2 for 48 h. Culture supernatants were removed and analyzed for the production of cytokines such as IFN-γ, TNF, and IL-17. Cytokine concentrations were determined using specific ELISAs (R&D Systems, Minneapolis, MN) as per the manufacturer's recommendations.

Isolation of NK cells and cytotoxicity assay

Spleen cell suspensions were prepared from $RAG^{-/-}$ or $IL\text{-}7^{-/-}RAG^{-/-}$ mice and treated with NH_4Cl buffer to remove erythrocytes. The NK cell population was then labeled with FITC-conjugated anti-DX5 (CD49b) and isolated for use as effector cells in the cytotoxicity assay by sorting on a FACSAria. The purity of isolated NK cells was 98.0% on reanalysis. To measure cytokine production, 5×10^4 NK cells were cultured in 200 μl RPMI 1640 supplemented with 10% FBS, 500 U/ml penicillin, and 100 μg/ml streptomycin in the presence of 100 ng/ml rIL-2, 100 ng/ml rIL-12, and 100 ng/ml rIL-18 on flat-bottom 96-well plates at 37°C in a humidified atmosphere incubator containing 5% CO_2. Culture supernatants were removed after 24 h and analyzed for IFN-γ production. Cytotoxicity assays were performed using the flow cytometric method reported by Xu et al. (28; see also Ref. 29). Briefly, isolated naive T cells from WT mice or LP effector memory T cells (T_{EM}) from colitic mice were labeled with a lipophilic green fluorescent cell linker, PKH2 (Sigma-Aldrich), which is incorporated into the plasma membrane. Uniform labeling of cells was confirmed by flow cytometry. Labeled 5×10^4 target T cells were coincubated in round-bottom 96-well plates (Costar) with effector NK cells (T:E ratio, 1:5 to 1:0.6) in complete RPMI 1640 supplemented with 100 ng/ml rIL-2 (PeproTech, London, U.K.) with or without 50 ng/ml rIL-7 (PeproTech) at 37°C in humidified air containing 5% CO_2 for 4 h. Naive T cells or LP colitogenic T cells that were incubated under the same conditions but without effector NK cells were also prepared as controls. Cells were then collected, stained with propidium iodide (PI), and analyzed by FACS. Cytotoxic activity was determined by calculating the percentage of the double-positive population for both PI (FL2) and PKH2 (FL1). In some experiments, a mouse lymphoma cell line, YAC-1, obtained from the American Type Culture Collection, was used as target cells for a [^{51}Cr] release assay with the standard protocol. Briefly, target cells were labeled with 3.7 MBq of $Na_2[^{51}Cr]O_4$ for 1 h at 37°C and washed three times with PBS before mixing (1×10^4/well) with effector cells in round-bottomed 96-well plates at different E:T ratios (1.25:1, 2.5:1, 5:1, 10:1, 20:1) in triplicates. After 4 h incubation, cell-free supernatants were collected and radioactivity measured by MicroBeta counter (Wallac). The percentage of lysis is calculated by (sample release − spontaneous release)/(maximum release − spontaneous release).

Statistical analysis

The results are expressed as the means ± SEM. Statistical significance was determined using the nonparametric Mann–Whitney U test, and differences were considered to be statistically significant when $p < 0.05$.

Results

NK cell depletion induces the early onset of colitis in naive T cell-transferred $RAG^{-/-}$ mice

It has been reported that NK cells suppress the severity of inflammatory diseases such as EAE and colitis (22, 24). NK cells were depleted in the latter colitis study by injection of anti-NK1.1 or anti-ASGM1 Abs, or by the use of a perforin-deficient animal. That study suggested that NK cells may possibly have cytolytic activity for colitogenic $CD4^+$ T_{EM} in this model since knockout of the perforin gene resulted in exacerbation of disease severity. However, it is unclear which stage in the development of colitis is affected by NK cells. Therefore, we first assessed the effect of NK cell depletion at different time points in the development of chronic colitis.

To examine the effect of NK cells in the development of chronic inflammation in the colon, an animal model of colitis was induced by adoptive transfer of $CD4^+CD62L^+D44^-$ (naive) T cells derived from WT SP into $RAG^{-/-}$ recipient mice (2, 3). NK cells were depleted by i.p. injection of the anti-ASGM1 Ab (or vehicle control [PBS]) every other day for 12 wk starting from the day before naive T cell transfer (Fig. 1A). Additionally, some groups were injected with the anti-ASGM1 Ab for 4 wk followed by vehicle control for 8 wk (Fig. 1A), or with the vehicle control for 4 wk followed by 8 wk anti-ASGM1 Ab (Supplemental Fig. 1). Mice injected with the anti-ASGM1 Ab for 12 wk, or for just the first 4 wk, started to show wasting earlier than the vehicle control group that was injected for 12 wk (Fig. 1B). Alternatively, mice injected with vehicle control for 4 wk followed by 8 wk anti-ASGM1 Ab showed a similar wasting curve to that of mice injected with vehicle control for 12 wk (data not shown), suggesting that NK cell depletion at the later stage of colitis induction does not affect the severity of colitis.

However, there was no significant difference in clinical scores between these groups 12 wk after the T cell transfer (Fig. 1C), and all mouse groups showed a similar degree of colitis with thickening and shortening of the colon as well as splenomegaly when sacrificed (Fig. 1D). Consistent with this finding, microscopic evaluation of each group showed similar histopathological features such as wall thickening of the colon, infiltration mainly by mononuclear cells, crypt abscesses, crypt elongation, a decrease in goblet cells, and epithelial damage (Fig. 1E, 1F). Moreover, the production of proinflammatory cytokines by colonic LP T cells isolated from each group was similar (Fig. 1G).

However, there was concern that anti-ASGM1 Ab treatment at an early stage may affect the colitis severity in the $RAG^{-/-}$ mice receiving naive T cells, since the groups with the Ab treatment at an early stage for 4 wk and 12 wk started to exhibit wasting earlier than the control group without the Ab treatment (Fig. 1B). Therefore, we examined these mice at a relatively early time and, interestingly, we found that the Ab-treated group showed significantly more severe colitis in clinical and histological scores compared with the control group 6 wk after T cell transfer (Fig. 2). These data indicate that NK cell depletion affects the early stage of colitis development.

$CD62L^-CD44^+$ and $CD62L^-CD44^-$ T cell subsets are increased by NK cell depletion in naive T cell-reconstituted $RAG^{-/-}$ recipient mice

Because the exacerbation at an early stage of colitis development was observed following NK cell depletion, we assessed the number of $CD4^+$ T cells in SPL and MLN of naive T cell-receiving $RAG^{-/-}$ mice treated with or without the anti-ASGM1 Ab. As seen in Fig. 3A and 3B, increased numbers of T cells were detected, especially

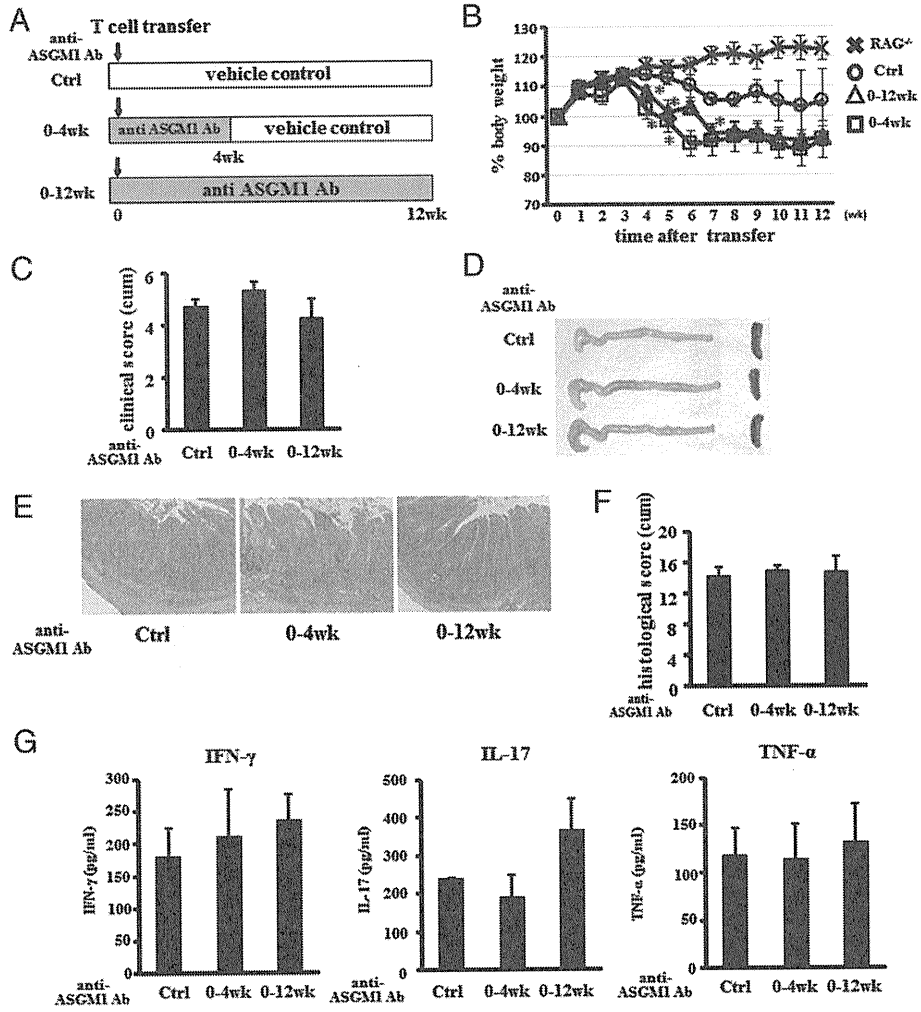

FIGURE 1. NK cell depletion at the early stage of colitis induction in $RAG^{-/-}$ mice results in wasting disease. (**A**) Protocol for NK cell depletion in a chronic colitis setting. $RAG^{-/-}$ mice were injected with either 0.25 mg/mouse anti-ASGM1 Ab (0–12 wk) or vehicle control (Ctrl) every second day for 12 wk from the day before adoptive transfer of naive T cells, or were injected with anti-ASGM1 Ab for 4 wk followed by vehicle control injection for 8 wk (0–4 wk). (**B**) Wasting, as defined by percentage of initial body weight, in $RAG^{-/-}$ mice induced colitis. Mice were injected with naive T cells and either vehicle control for 12 wk (Ctrl, ○), anti-ASGM1 Ab for 12 wk (0–12 wk, △), or anti-ASGM1 Ab for 4 wk followed by 8 wk vehicle control (0–4 wk, □). The non–T cell-injected control group is also shown ($RAG^{-/-}$, cross). Data are expressed as means ± SEM from four mice. $*p < 0.05$. (**C**) Clinical scores of each group are shown. Data are expressed as means ± SEM from four mice. (**D**) Gross appearance of colons (*left*) and SP (*right*) from naive T cell-transferred $RAG^{-/-}$ recipients injected with either vehicle control for 12 wk (Ctrl, *top*), anti-ASGM1 Ab for 4 wk and then control for 8 wk (0–4 wk, *middle*), or anti-ASGM1 Ab for 12 wk (0–12 wk, *bottom*). Representative features from four experiments are shown. (**E**) Histological feature of colons from naive T cell-transferred $RAG^{-/-}$ recipients injected with control for 12 wk (Ctrl, *left*), anti-ASGM1 Ab for 4 wk and then control for 8 wk (0–4 wk, *middle*), or anti-ASGM1 Ab for 12 wk (0–12 wk, *right*). Representative features from each group are shown. (**F**) Histological scores of each group are shown. Data are expressed as means ± SEM from four mice. (**G**) Cytokine production by LP T cells from each group is shown. Concentrations of IFN-γ (*left*), TNF (*middle*), and IL-17 (*right*) in the culture supernatant were measured using ELISA. Data are indicated as means ± SEM from four samples.

in the SPL, within a week after naive T cell injection. Moreover, treatment with the anti-ASGM1 Ab revealed a significantly increased number of T cells in SPL and MLN (Fig. 3A, 3B). Thus, we next determined the development of T_{EM} in these mice by assessment of the expression levels of CD62L and CD44 on T cells. From day 1 to day 3, most T cells still expressed CD62L, but not CD44, regardless of anti-ASGM1 Ab treatment. Interestingly, a $CD62L^{-}CD44^{-}$ subset had appeared in both SPL and MLN by day 5 after treatment with anti-ASGM1 Ab (Fig. 3C–F). This unique T cell subset was significantly increased in the naive T cell-receiving $RAG^{-/-}$ mice treated with anti-ASGM1 Ab, especially in MLN, on days 5 and 7 (Fig. 3F), suggesting that NK cells target this $CD62L^{-}CD44^{-}$ T cell subset upon development of colitogenic $CD62L^{-}CD44^{+}$ T_{EM}.

It is thought that the T_{EM}, but not a naive T cell subset, is targeted by NK cells to regulate excessive immune responses (23, 28). However, our observation indicated that a $CD62L^{-}CD44^{-}$ T cell subset is increased in the absence of NK cells. Therefore, we next assessed the expression levels of several markers, which are associated with NK cell function, on each of the T cell subsets. Splenic $CD62L^{+}CD44^{-}$ (naive, R1; Fig. 4, *left panel*), $CD62L^{-}CD44^{-}$ (R2), and $CD62L^{-}CD44^{+}$ (effector memory, R3) T cell subsets were isolated for FACS analysis from $RAG^{-/-}$ mice that had received naive T cells 5 d previously with anti-ASGM1 Ab treatment the day before T cell reconstitution. The expression of Fas and DR5 in $CD62L^{-}CD44^{+}$ cells was higher than that in $CD62L^{+}CD44^{-}$ T cells (Fig. 4). Interestingly, the expression levels of Fas and DR5 in $CD62L^{-}CD44^{-}$ cells were similar to those of $CD62L^{+}CD44^{-}$, but not of $CD62L^{-}CD44^{+}$. Additionally, the expression level of Qa-1 was similar for all of these T cell subsets (Fig. 4). Furthermore, the expression level of IL-7R/CD127 in $CD62L^{-}CD44^{+}$ cells was similar to that of $CD62L^{+}$

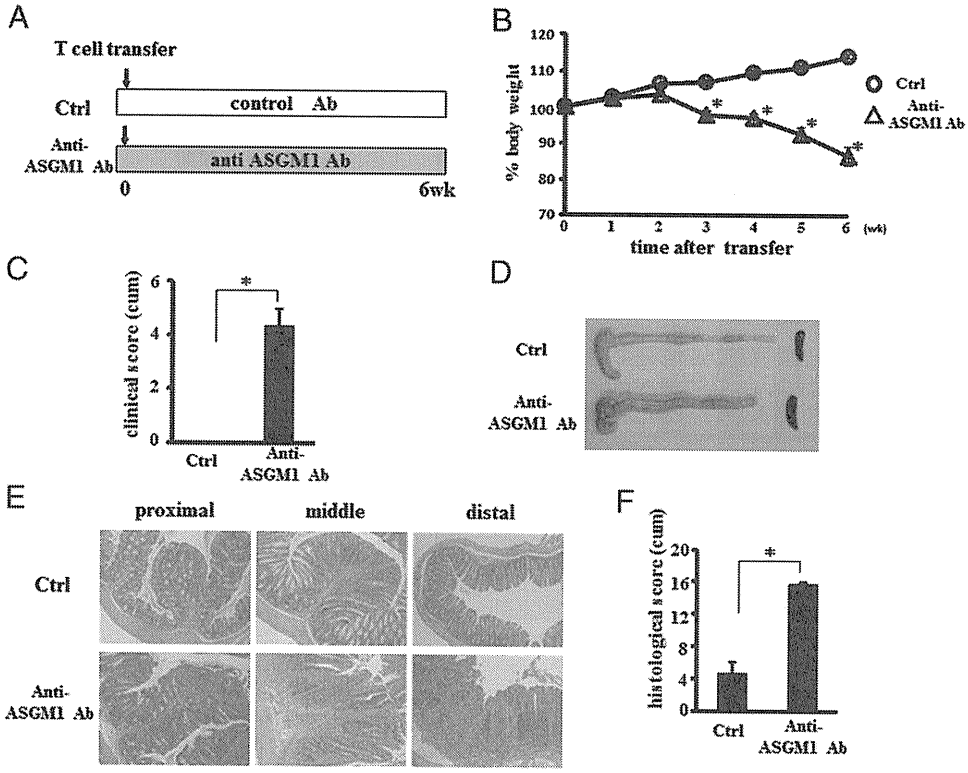

FIGURE 2. NK cell depletion in $RAG^{-/-}$ recipients results in early onset colitis development. (**A**) Protocol for NK cell depletion in a chronic colitis setting. $RAG^{-/-}$ mice were injected with either 0.25 mg/mouse anti-ASGM1 Ab or control IgG every second day for 6 wk from the day before adoptive transfer of naive T cells. (**B**) Wasting, as defined by percentage of initial body weight, in $RAG^{-/-}$ mice induced colitis. Mice were injected with naive T cells with either control IgG (○) or anti-ASGM1 Ab (△) for 6 wk. Data are expressed as means ± SEM from four mice. $*p < 0.05$. (**C**) Clinical scores of each group are shown. Data are expressed as means ± SEM from four mice. $*p < 0.05$. (**D**) Gross appearance of colons (*left*) and SP (*right*) from naive T cell-transferred $RAG^{-/-}$ recipients injected with either control IgG (*top*) or anti-ASGM1 Ab for 6 wk (*bottom*). Representative features from four experiments are shown. (**E**) Histological feature of proximal (*left*), middle (*middle*), and distal (*right*) colons from naive T cell-transferred $RAG^{-/-}$ recipients injected with either control IgG (*top*) or anti-ASGM1 Ab for 6 wk (*botttom*). Representative features from each group are shown. (**F**) Histological scores of each group are shown. Data are expressed as means ± SEM from four mice. $*p < 0.005$.

$CD44^-$ cells. Most $CD62L^-CD44^-$ cells showed a similar IL-7R/CD127 expression level to the other subsets; however, some cells within this subset showed a lower expression of the IL-7R as seen in Fig. 4 (arrow). These results indicate that the mechanism by which NK cells suppress $CD62L^-CD44^-$ T cells may be different from that by which they suppress T_{EM}, which is due to NK cell-induced apoptosis via Fas and/or DR5.

The lack of IL-7 does not affect the cytotoxic activity of NK cells

Because we have previously observed the upregulated annexin V and downregulated Bcl-2 expressions in the $CD4^+$ T cells transferred into $IL\text{-}7^{-/-}RAG^{-/-}$ recipients (10), we speculated that the ability of NK cells to suppress the T cells could be affected by the presence or absence of IL-7. We therefore performed a cytotoxicity assay to test this hypothesis. As expected, NK cells (effector) had negligible cytotoxicity toward $CD62L^+CD44^-$ naive T cells (target) derived from WT SP (T:E ratio, 1:5) regardless of whether rIL-7 was present (Fig. 5A). When $CD62L^-CD44^+$ T_{EM} derived from colonic LP of $RAG^{-/-}$ mice, which had been injected with naive T cells 12 wk previously, were coincubated with the NK cells (T:E ratio, 1:5), the mortality of the target cells was elevated but this cell-mediated cytotoxicity did not change in the presence of rIL-7 (Fig. 5B). These results suggested that the cytotoxic ability of NK cells derived from WT mice was not affected by IL-7 and further suggested that the susceptibility of T cells to the cytotoxic activity of NK cells was not changed by the presence of IL-7 using this assay. When increasing the ratio of $CD62L^-$ $CD44^+$ T_{EM} (T:E ratio, 1:5 to 1:0.6), the mortality was decreased (Fig. 5C). These data suggest that the cytotoxicity is decreased when the number of target T cells exceeds the capacities of effector NK cells to suppress T cells. However, it was still unclear whether the cytotoxic ability of NK cells could be modulated during its development in vivo in the presence or absence of IL-7. Therefore, the cytotoxic ability of NK cells derived from $RAG^{-/-}$ and $IL\text{-}7^{-/-}$ $RAG^{-/-}$ mice was examined. As seen in Fig. 5D, there was little mortality of $CD62L^+$ $CD44^-$ naive T cells alone, and this mortality was unaffected even if coincubated with NK cells derived from either $RAG^{-/-}$ or $IL\text{-}7^{-/-}RAG^{-/-}$ mice (T:E ratio, 1:5). The mortality of $CD62L^-CD44^+$ T_{EM} was elevated compared with that of T_{EM} alone when coincubated with NK cells derived from $RAG^{-/-}$ mice and was similar to that following coincubation with NK cells derived from $IL\text{-}7^{-/-}RAG^{-/-}$ mice (T:E ratio, 1:5; Fig. 5E).

Additionally, the expression levels of NK receptors (30) that reflect the function of NK cells (Fig. 5F), as well as the levels of CD11b and CD27 that determine the differentiation status of NK cells (31) (Fig. 5G), were not altered in NK cells derived from $IL\text{-}7^{-/-}RAG^{-/-}$ mice, compared with those from $RAG^{-/-}$ mice.

To further demonstrate that there are no differences of NK cell functions between $RAG^{-/-}$ and $IL\text{-}7^{-/-}RAG^{-/-}$, we also measured the cytotoxic activities of these cells against YAC-1 cells using the [^{51}Cr] release assay, as well as the production of IFN-γ from these cells. As seen in Fig. 5H and 5I, neither the cytotoxicities against YAC-1 cells nor IFN-γ production of NK cells was modified in the $IL\text{-}7^{-/-}RAG^{-/-}$ mice when compared with

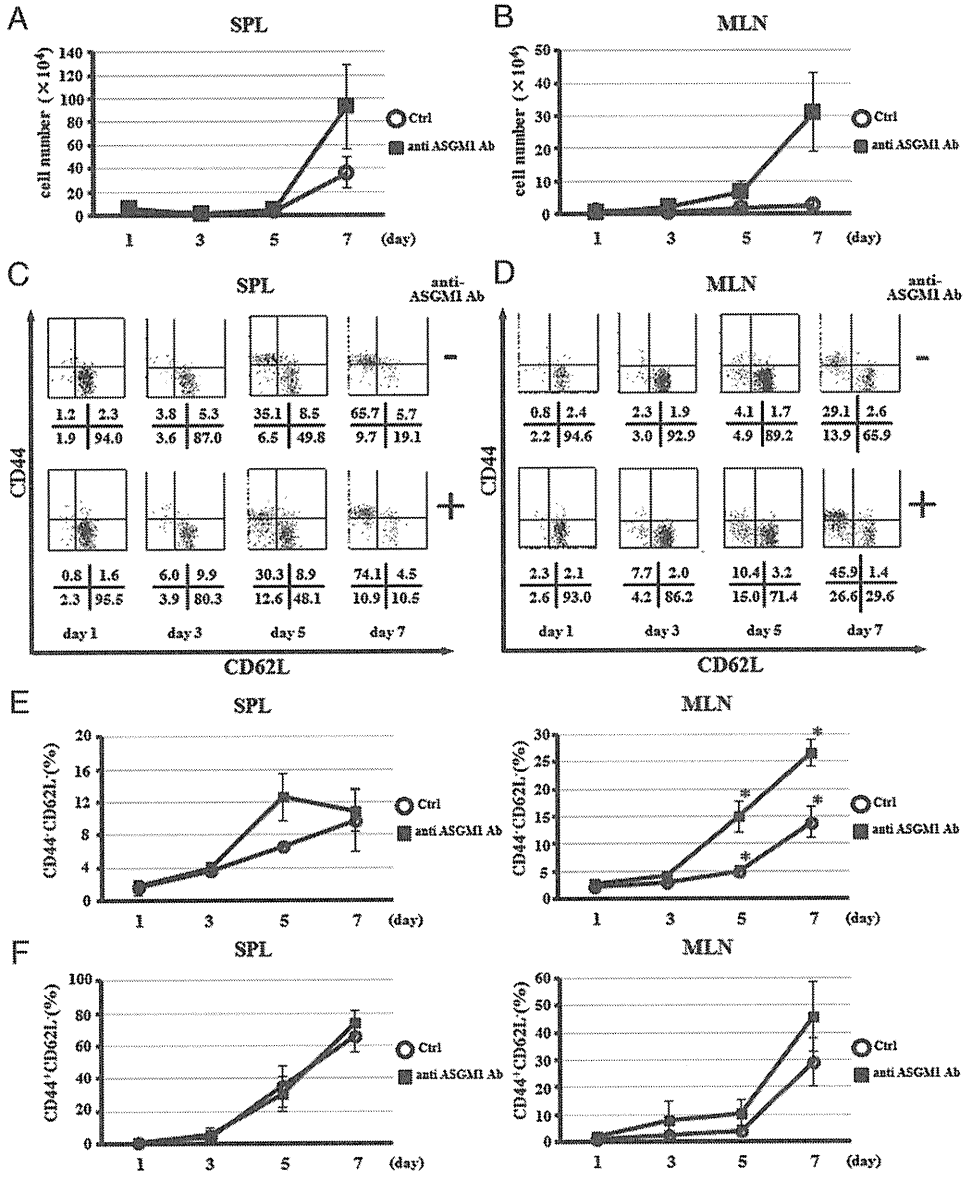

FIGURE 3. NK cell depletion results in the increase in $CD44^+CD62L^-$ and $CD44^-CD62L^-$ subsets in naive T cell-transferred $RAG^{-/-}$ mice. (**A** and **B**) Naive T cells derived from WT SP were adoptively transferred into $RAG^{-/-}$ mice that were preinjected with either vehicle control (○) or anti-ASGM1 Ab (■). Mice were sacrificed and the total number of $CD4^+$ T cells isolated from SP (A) or MLN (B) was counted. Cells were stained with PerCP-conjugated anti-CD3 and allophycocyanin-conjugated anti-CD4 Abs, and were then subjected to FACS to calculate the number of T cells in each sample. The number of $CD4^+$ T cells at the indicated time points is shown. Data are expressed as means ± SEM ($n = 4$). (**C** and **D**) The naive T cell-receiving $RAG^{-/-}$ mice that had been preinjected with either vehicle control or anti-ASGM1 Ab were sacrificed at the indicated time points after naive T cell transfer. The isolated lymphocytes from SP (C) or MLN (D) were stained with allophycocyanin-conjugated anti-CD4, PerCP-conjugated anti-CD3, FITC-conjugated anti-CD62L, and PE-conjugated anti-CD44 Abs and were subjected to FACS. Representative data from four experiments are shown. The numbers in each data quadrant indicate percentage of gated populations. (**E** and **F**) The percentage of $CD44^-CD62L^-$ cells in $RAG^{-/-}$ mice that received naive T cells with or without anti-ASGM1 Ab injection. Mice were sacrificed at the indicated time points, lymphocytes isolated from SP (E) or MLN (F) were stained with anti-CD3, anti-CD4, anti-CD62L, and anti-CD44 Abs and were then subjected to FACS to analyze the percentage of the subset. Data are expressed as means ± SEM from five experiments. $^*p < 0.05$.

$RAG^{-/-}$ mice. These results confirm that a lack of IL-7 does not affect the cytotoxic activity of NK cells either in vitro or in vivo.

K cell depletion elicits severe colitis in naive T cell-transferred IL-7$^{-/-}$ RAG$^{-/-}$ recipient mice

We previously reported that the development of colitis is abrogated by a lack of IL-7. Given that NK cells can suppress T cells in vitro and in vivo independently of IL-7, we next assessed the influence of NK cells on colitis in the context of IL-7 deficiency in vivo. IL-$7^{-/-}$ $RAG^{-/-}$ mice were injected i.p. with naive T cells with or without anti-ASGM1 Ab treatment, and colitis was monitored after 12 wk (Fig. 6A). As previously observed, the induction of colitis was completely abrogated in vehicle control-injected IL-$7^{-/-}RAG^{-/-}$ mice, as shown by clinical and histological scores and cytokine production from colonic LP lymphocytes, although the presence of occasional leukocytes was observed in colonic tissues (Fig. 6B–E). However, when anti-ASGM1 Ab was injected, IL-$7^{-/-}RAG^{-/-}$ mice showed elicitation of colitis and similar severity of clinical phenotypes, such as wasting and diarrhea, as did the groups of $RAG^{-/-}$ recipients with or without anti-ASGM1 Ab treatment (Fig. 6B). Consistent with these findings, a significant deterioration in histological findings, such as mucosal damage, cell infil-

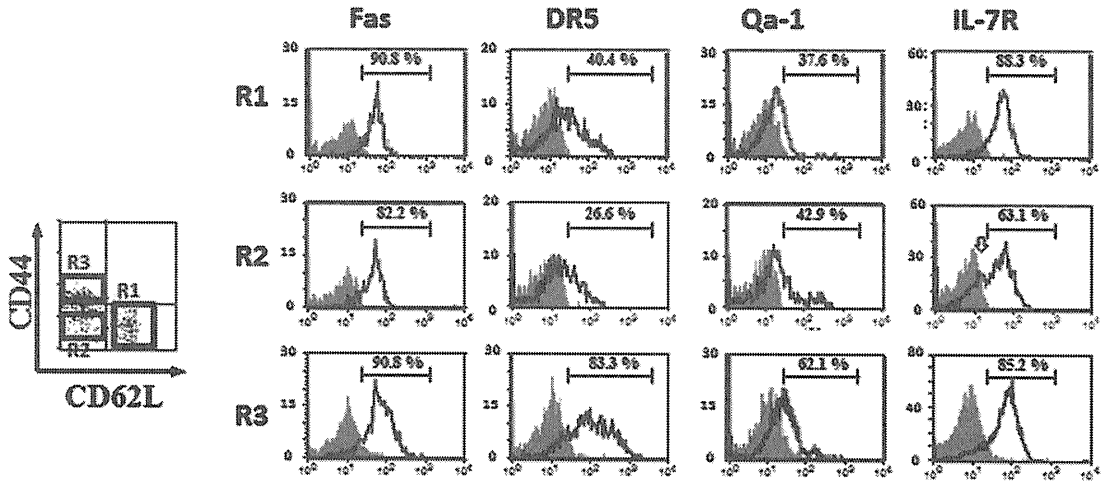

FIGURE 4. NK cells may target the $CD62L^-CD44^-$ subset by a different mechanism from that by which they target the $CD62L^-CD44^+$ subset. $RAG^{-/-}$ mice preinjected with anti-ASGM1 Ab were sacrificed 5 d after naive T cell transfer. Isolated splenocytes were stained with anti-CD62L, anti-CD44, and either anti-Fas, anti-DR5, anti-Qa1, or anti-CD127 Abs (open histograms) or isotype-matched control (filled histograms) and were then subjected to FACS. The populations within the appropriate gate on forward scatter and side scatter and either $CD62L^+CD44^-$ (naive, R1), $CD62L^-CD44^-$ (R2) or $CD62L^-CD44^+$ (T_{EM}, R3) were analyzed. Representative data from three experiments are shown.

tration, and crypt abscesses, was also observed in $IL\text{-}7^{-/-}RAG^{-/-}$ mice when treated with anti-ASGM1 Ab (Fig. 6C, 6D) in association with the exacerbation in the clinical scores of these mice. Moreover, the production of cytokines such as IFN-γ, TNF-α, and IL-17 by colonic LPL from anti-ASGM1 Ab-treated $IL\text{-}7^{-/-}RAG^{-/-}$ mice was significantly upregulated when compared with the vehicle control-treated group, despite the fact that their production was relatively lower than that of $RAG^{-/-}$ groups with or without anti-ASGM1 Ab treatment (Fig. 6E). These results suggest that severe inflammation occurs in colonic tissues following NK cell depletion even in $IL\text{-}7^{-/-}RAG^{-/-}$ mice.

Additionally, to confirm the activities of cells that had infiltrated the tissues, absolute numbers of splenic and colonic LP $CD4^+$ T cells isolated from these colitic mice were calculated (Fig. 7A) and analyzed by FACS (Fig. 7B, 7C). As seen in Fig. 7B and 7C, the percentage of $NK1.1^+$ cells in both SP and colonic LP was greatly decreased in T cell-reconstituted mice treated with anti-ASGM1 Ab. Note that the percentages of $NK1.1^+$ populations in both SP and colonic LP from T cell-reconstituted $IL\text{-}7^{-/-}RAG^{-/-}$ mice not treated with the anti-ASGM1 Ab were dramatically increased, because there were less $CD4^+$ T cells in the tissues (Fig. 7A). Additionally, $CD4^+$ T cells with a $CD44^+CD62L^-$ phenotype were observed in all mouse groups (Fig. 7B, 7C). However, the percentage of these cells was lower, especially in colonic LP, in $IL\text{-}7^{-/-}RAG^{-/-}$ recipient mice not treated with the anti-ASGM1 Ab relative to the other groups. Associated with this finding, the expression levels of IL-7R and CD69 in both splenic and colonic LP $CD4^+$ T cells from $IL\text{-}7^{-/-}RAG^{-/-}$ recipient mice not treated with the anti-ASGM1 Ab were downregulated relative to the other groups (Fig. 7B, 7C). However, treatment with the anti-ASGM1 Ab resulted in an increase in $CD4^+CD44^+CD62L^-$ T cells in both splenic and colonic LP, as well as upregulation of the expression of IL-7R and CD69 in $IL\text{-}7^{-/-}RAG^{-/-}$ recipient mice. These results indicate that the T cells reconstituted into $IL\text{-}7^{-/-}RAG^{-/-}$ recipient mice are still able to survive even 12 wk after injection, but that they somehow fail to differentiate sufficiently to induce colitis. Moreover, these data suggest that the depletion of NK cells in this context may assist the T cells to establish themselves as pathogenic T cells.

To further confirm whether such elicitation of pathogenic T cells in $IL\text{-}7^{-/-}RAG^{-/-}$ recipients was induced by NK cell depletion, anti-NK1.1 Ab was used for the same model. $IL\text{-}7^{-/-}RAG^{-/-}$ mice were injected i.p. with naive T cells with or without anti-NK1.1 Ab treatment, and colitis was monitored after 12 wk (Fig. 8A). The $IL\text{-}7^{-/-}RAG^{-/-}$ recipients injected with anti-NK1.1 Ab showed severe colitis (Fig. 8B–D) with increased production of proinflammatory cytokines by the colonic LPL when compared with the isotype control-injected mice (Fig. 8E). These results suggested that the phenotypes shown in $IL\text{-}7^{-/-}RAG^{-/-}$ recipients may reflect NK cell regulation of T cell development in this model.

NK cell depletion at an early stage is critical for the induction of colitis in naive T cell-transferred $IL\text{-}7^{-/-}RAG^{-/-}$ recipient mice

Because NK cell depletion resulted in the exacerbation of colitis even in $IL\text{-}7^{-/-}RAG^{-/-}$ recipient mice, we finally examined the effect of NK cell depletion at early and late stages of colitis development in $IL\text{-}7^{-/-}RAG^{-/-}$ recipient mice. Mice receiving naive T cells were also injected every 48 h with either the vehicle control for 12 wk (Ctrl), anti-ASGM1 Ab for 12 wk (0–12 wk), anti-ASGM1 Ab for 4 wk followed by vehicle control for 8 wk (0–4 wk), or vehicle control for 4 wk followed by 8 wk anti-ASGM1 Ab (4–12 wk), and colitis was monitored after 12 wk (Fig. 9A). Mice injected with anti-ASGM1 Ab for the first 4 wk, or for the entire 12 wk, showed significantly more severe clinical phenotypes of colitis than did the other groups (Fig. 9B), which was associated with thickening and shortening of the colon and splenomegaly (Fig. 9C). Severe inflammation of the colon, as judged by histological analysis, was also noticeably induced in these two groups (Fig. 9D, 9E). However, mice injected with the anti-ASGM1 Ab at a later stage failed to induce colitis, although minor clinical symptoms and infiltration of a few cells into the colon were occasionally observed (Fig. 9B–E). Moreover, these degrees of severity of colitis were consistent with cytokine production from colitic LP T cells, since significantly upregulated IFN-γ and TNF-α production was observed in the groups treated with the anti-ASGM1 Ab either at the beginning or throughout the entire period, but not in the group treated with the Ab only at the later stage (Fig. 9F). Note that the level of IL-17 production in mice treated for the entire period with anti-ASGM1 Ab was significantly higher than that of mice treated with the Ab only at the

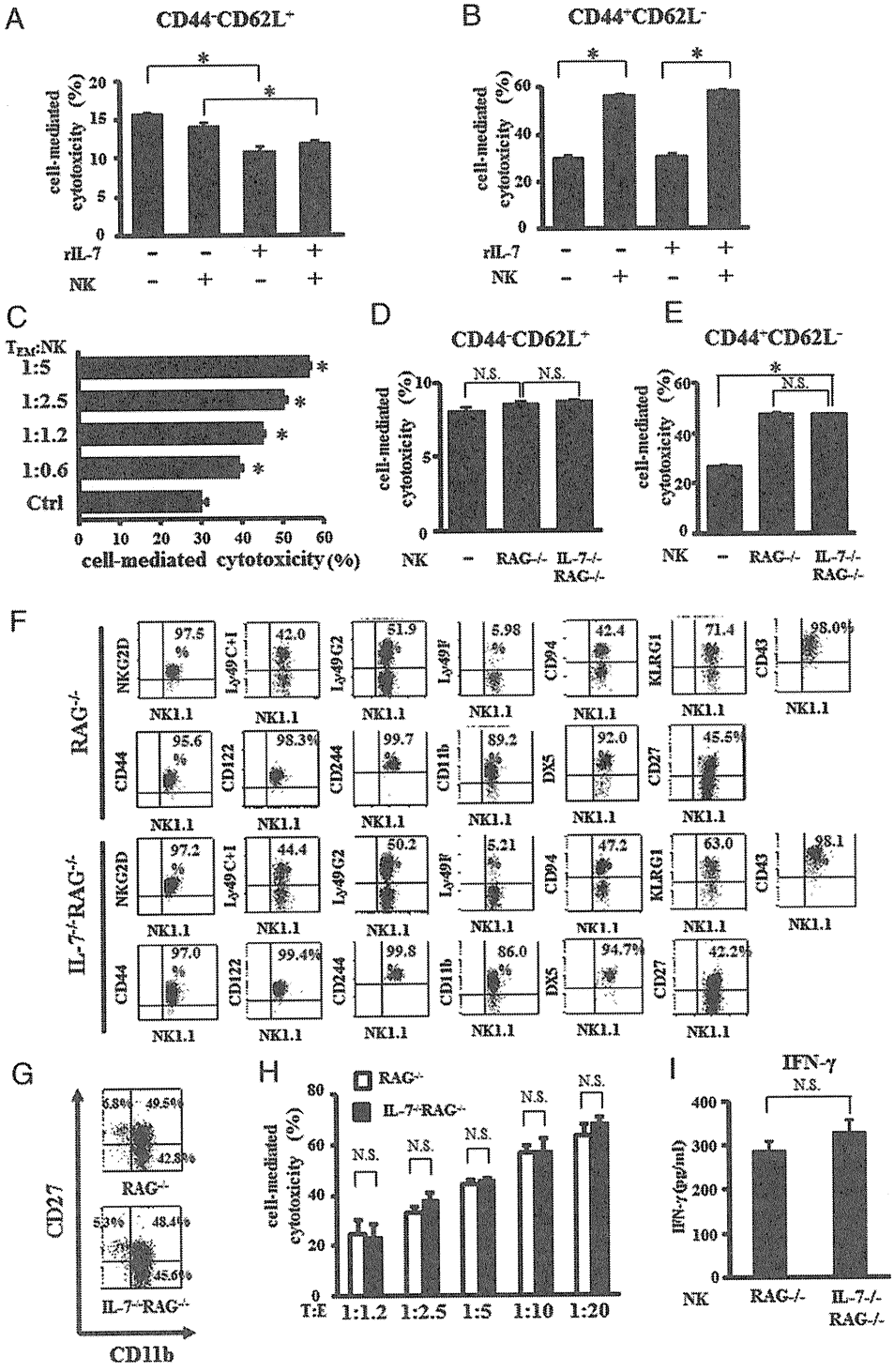

FIGURE 5. Cytotoxic activity of NK cells is not affected in the presence or absence of IL-7. (**A–C**) Splenic NK cells were isolated from WT mice by FACS sorting. Either $CD4^+CD62L^+CD44^-$ naive T cells isolated from WT SP (A) or $CD4^+CD62L^-CD44^+$ T_{EM} from colonic LP in $RAG^{-/-}$ mice that received naive T cells 12 wk previously (B and C) were stained with PKH2 and cocultured as target (T) cells with the isolated NK cells as effector (E) cells, in the presence or absence of IL-7 for 4 h. Cells were then harvested and stained with PI. The PKH2 and PI double-positive population is assumed to represent dead target cells (28). The mortality of target cells was calculated as the ratio of dead $PKH2^+$ cells. (A) T:E ratio, 1:5, with or without rIL-7; (B) T:E ratio, 1:5, with or without rIL-7; (C) T:E ratio, 1:5, 1:2.5, 1:1.25, or 1:0.625, without rIL-7. Control ($CD4^+$ T cells alone) is also shown as a negative control. Data are expressed as means ± SEM from three experiments. $^*p < 0.001$. (**D** and **E**) Splenic NK cells were isolated from either $RAG^{-/-}$ or $IL\text{-}7^{-/-}$ $RAG1^{-/-}$ mice by FACS sorting. Either the $CD62L^+CD44^-$ naive T (D) or the $CD62L^-CD44^+$ T_{EM} (E) subset was stained with PKH2 and cocultured for 4 h with splenic NK cells derived from either $RAG^{-/-}$ or $IL\text{-}7^{-/-}RAG1^{-/-}$ mice. Cells were then stained with PI and subjected to the cytotoxic assay described above. Data are expressed as means ± SEM from three experiments. $^*p < 0.001$. (**F**) Splenic NK cells were isolated from $RAG^{-/-}$ and $IL\text{-}7^{-/-}$ $RAG^{-/-}$ mice, and the expression of each NK receptor on these cells was assessed by FACS. The numbers indicate the percentage of cells positive for each NK receptor in the NK1.1-positive population. (**G**) Splenic NK cells isolated from either $RAG^{-/-}$ or $IL\text{-}7^{-/-}RAG^{-/-}$ mice were stained with anti-CD11b and anti-CD27 Abs and were then subjected to FACS to evaluate their differentiation status. The numbers indicate the quadrant percentages of each differentiation status in the NK1.1-positive population. (**H**) Splenic NK cells were isolated from $RAG^{-/-}$ (open) and $IL\text{-}7^{-/-}$ $RAG^{-/-}$ (filled) mice by FACS sorting. YAC-1 cells were labeled with $Na_2[^{51}Cr]O_4$ and cocultured as target (T) cells with the isolated NK cells as *(Figure legend continues)*

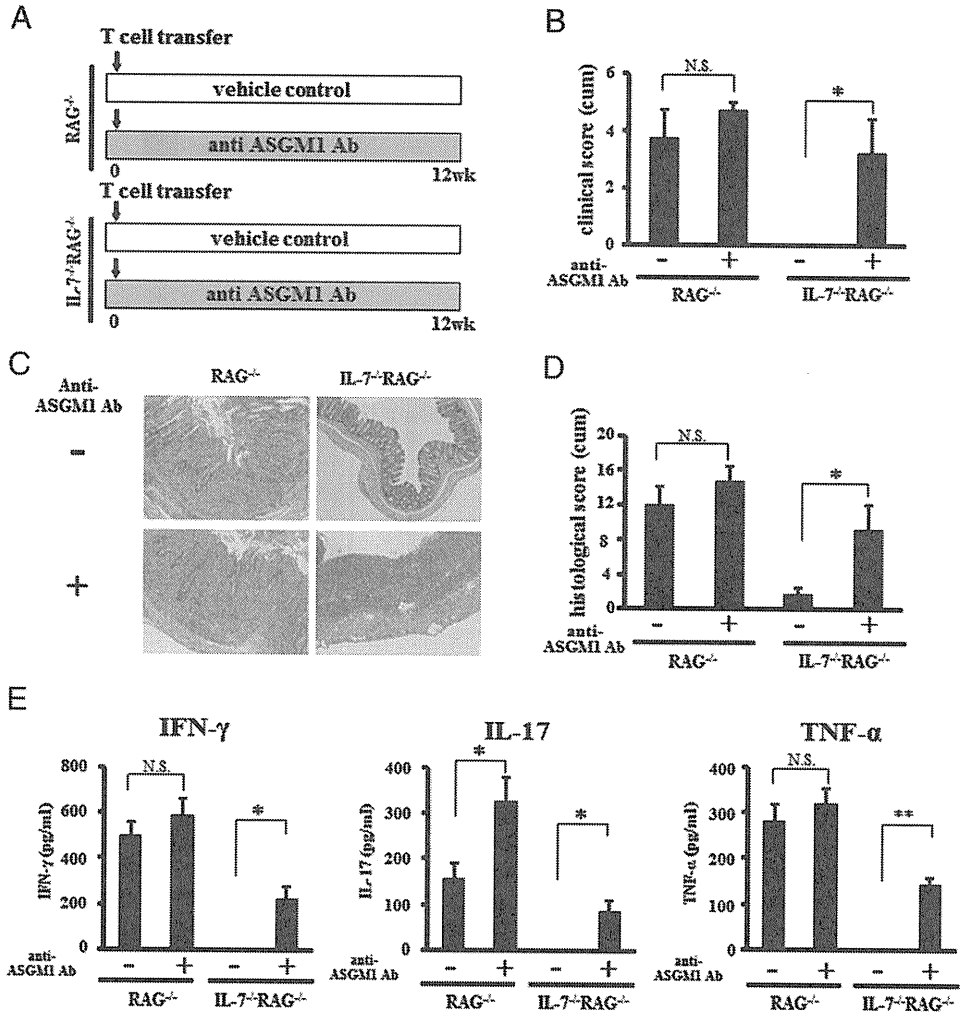

FIGURE 6. NK cell depletion with anti-ASGM1 Ab in naive T cell-receiving IL-$7^{-/-}$$RAG^{-/-}$ mice, as well as in $RAG^{-/-}$ recipients, results in the development of colitis. (**A**) Protocol for NK cell depletion in a colitis setting. Naive T cell-receiving $RAG^{-/-}$ and IL-$7^{-/-}$$RAG^{-/-}$ mice were injected with either anti-ASGM1 Ab (0–12 wk) or vehicle control (Ctrl) every second day for 12 wk starting from the day before adoptive transfer of naive T cells. (**B**) Clinical scores of each group are shown. Data are expressed as means ± SEM from four mice. *$p <$ 0.05. (**C**) Histological features of colons from naive T cell-transferred $RAG^{-/-}$ and IL-$7^{-/-}$$RAG^{-/-}$ recipients injected with either vehicle control (Ctrl) or anti-ASGM1 for 12 wk (0–12 wk). Representative features from four experiments are shown. (**D**) Histological scores of each group are shown. Data are expressed as means ± SEM from four mice. *$p < 0.05$. (**E**) Cytokine production by LP T cells from each group is shown. Concentrations of IFN-γ (*left*), TNF (*middle*), and IL-17 (*right*) in the culture supernatant are measured by ELISA. Data are indicated as means ± SEM from four samples. *$p < 0.05$, **$p <$ 0.01.

beginning (Fig. 9F), although there was no significant difference in either clinical or histological scores between these groups (Fig. 9B, 9E). These results suggest that NK cell depletion at the early stage, but not the late stage, of T_{EM} development is critical for the induction of colitis in IL-$7^{-/-}$$RAG^{-/-}$ recipient mice.

Discussion

We previously reported that adoptively transferred WT naive T cells injected into IL-$7^{-/-}$$RAG^{-/-}$ mice interestingly failed to induce colitis (10). However, it is known that IL-7 is not required for the in vitro differentiation of naive T cells into Th1 or Th17 cells (12). We therefore speculated that the reason why the IL-$7^{-/-}$$RAG^{-/-}$ mice that received naive T cells failed to maintain colitogenic $CD4^+$ T_{EM} may be associated not only with a lack of IL-7, but also with another mechanism that involves suppression of the primary stage of T_{EM} development in the recipients. We previously reported that apoptosis is preferentially induced in $CD4^+$ T cells when IL-7 is lacking in vivo. Thus, increased numbers of annexin V^+CD4^+ T cells were observed in IL-$7^{-/-}$$RAG^{-/-}$ recipient mice, into which these T cells had been adoptively transferred, compared with $CD4^+$ T cells in $RAG^{-/-}$ recipient mice (10). These data suggested that T cell suppression via apoptosis is a mechanism by which colitis is abrogated in IL-$7^{-/-}$$RAG^{-/-}$ recipient mice. We therefore determined whether NK cells, which are known to induce apoptosis in $CD4^+$ T cells, may play a role in such T cell suppression.

Several reports have suggested that NK cells suppress the inflammation caused by autoimmune responses not only in animal models such as EAE and collagen-induced arthritis, but also in clinical samples from patients with multiple sclerosis and systemic lupus erythematosus in humans (20–22, 28, 32, 33). For example, depletion of NK cells using Abs against NK1.1 or ASGM1 results in disease exacerbation in the EAE model (22, 28). Additionally, it has also been reported that NK cell depletion exacerbates an animal model of colitis, although the details underlying the mechanism have not been elucidated (24).

In the present study, NK cells were depleted in the naive T cell adoptively transferred colitis model to analyze the role of NK cells in this model. $RAG^{-/-}$ and IL-$7^{-/-}$$RAG^{-/-}$ mice that had received naive T cells were depleted of NK cells using an anti-ASGM1 (Figs. 1, 2, 6, 9, Supplemental Figs. 1, 2). However, it was of concern that ASGM1 may be expressed not only in NK cells but also in some subsets of T cells and macrophages when activated (34). Therefore, we also administered anti-NK1.1 Ab

effector (E) cells for 4 h. T:E ratio, 1:20, 1:10, 1:5, 1:2.5, or 1:1.25. Data are expressed as means ± SEM from three experiments. (**I**) Cytokine production by NK cells from each group is shown. Concentrations of IFN-γ in the culture supernatant are measured by ELISA. Data are indicated as means ± SEM from four samples.

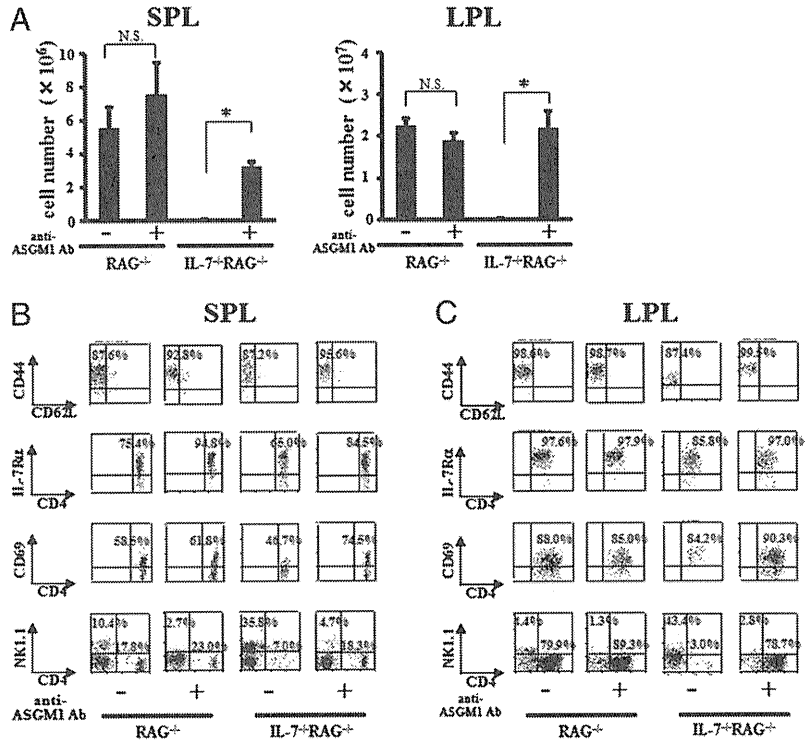

FIGURE 7. Colitogenic T_{EM} are induced in naive T cell-receiving IL-$7^{-/-}$RAG$^{-/-}$ by NK cell depletion. (**A**) Absolute numbers of $CD4^+$ T cells are shown. $CD4^+$ SPL (*left*) or colonic LPL (*right*) were isolated from naive T cell-receiving RAG$^{-/-}$ and IL-$7^{-/-}$ RAG$^{-/-}$ mice injected with either vehicle control (−) or anti-ASGM1 Ab (+) for 12 wk. Data are expressed as means ± SEM from five mice. *$p < 0.001$. (**B** and **C**) Isolated SPL (B) or colonic LPL (C) were stained with anti-CD4 and either anti-CD44, anti-CD127/IL-7Rα, anti-CD69, or anti-NK1.1 Abs and were then subjected to FACS analysis. Representative data from four experiments are shown.

using another experimental approach to confirm that the phenotypes shown in this model were induced by NK cell depletion (Fig. 8). Note that administration of anti-ASGM1 without T cell reconstitution to the IL-$7^{-/-}$RAG$^{-/-}$ mice does not trigger any inflammation in the colon (Supplemental Fig. 2). Also note that the appropriate controls, such as the same amount of rabbit Ig as a control for anti-ASGM1 polyclonal Ab and mouse IgG2a as an isotype-matched control for anti-NK1.1 (PK136), respectively, do not induce colitis in the recipients either (Figs. 2, 8, Supplemental Fig. 2). Interestingly, NK cell depletion at an early stage during colitis induction resulted in exacerbated colitis in the recipient, even in IL-$7^{-/-}$ RAG$^{-/-}$ recipient mice, in association with increased clinical and histological scores as well as upregulated cytokine production by colonic LP T cells. We observed strong

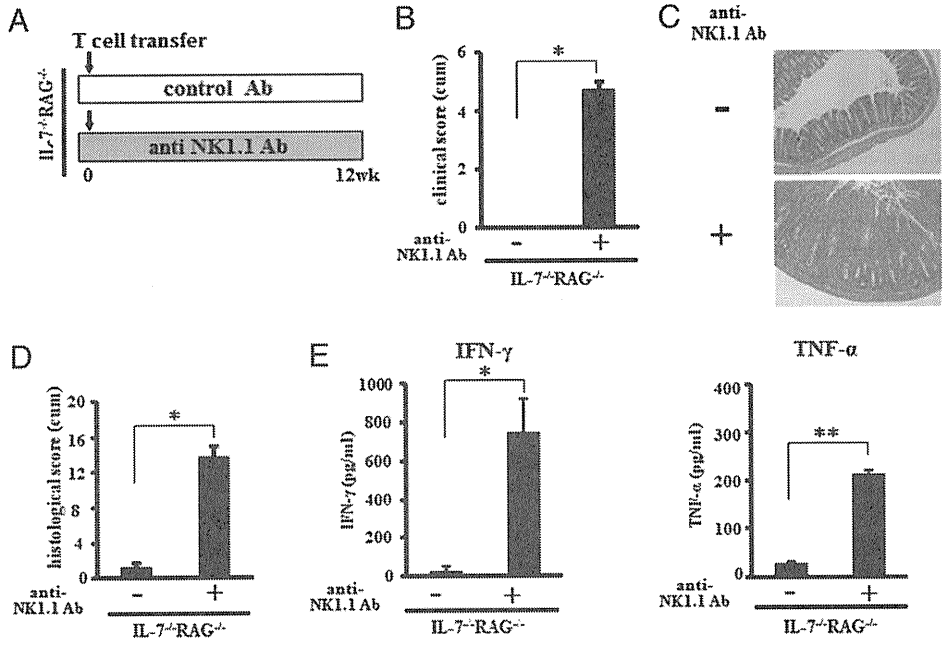

FIGURE 8. NK cell depletion with anti-NK1.1 Ab in naive T cell-receiving IL-$7^{-/-}$RAG$^{-/-}$ mice results in the elicitaion of colitis. (**A**) Protocol for NK cell depletion in a chronic colitis setting. IL-$7^{-/-}$RAG$^{-/-}$ mice receiving naive T cells were injected with either 0.5 mg/mouse anti-NK1.1 Ab or isotype control every second day for 12 wk. (**B**) Clinical scores of each group are shown. Data are expressed as means ± SEM from five mice. *$p < 0.001$. (**C**) Histological feature of colons from naive T cell-transferred IL-$7^{-/-}$RAG$^{-/-}$ recipients injected with isotype control (−, *top*) or anti-NK1.1 Ab (+, *bottom*). Representative features from each group are shown. (**D**) Histological scores of each group are shown. Data are expressed as means ± SEM from five mice. *$p < 0.001$. (**E**) Cytokine production by LP T cells from each group is shown. Concentrations of IFN-γ (*left*) and TNF-α (*right*) in the culture supernatant were measured by ELISA. Data are indicated as means ± SEM from five samples. *$p < 0.05$, **$p < 0.001$.

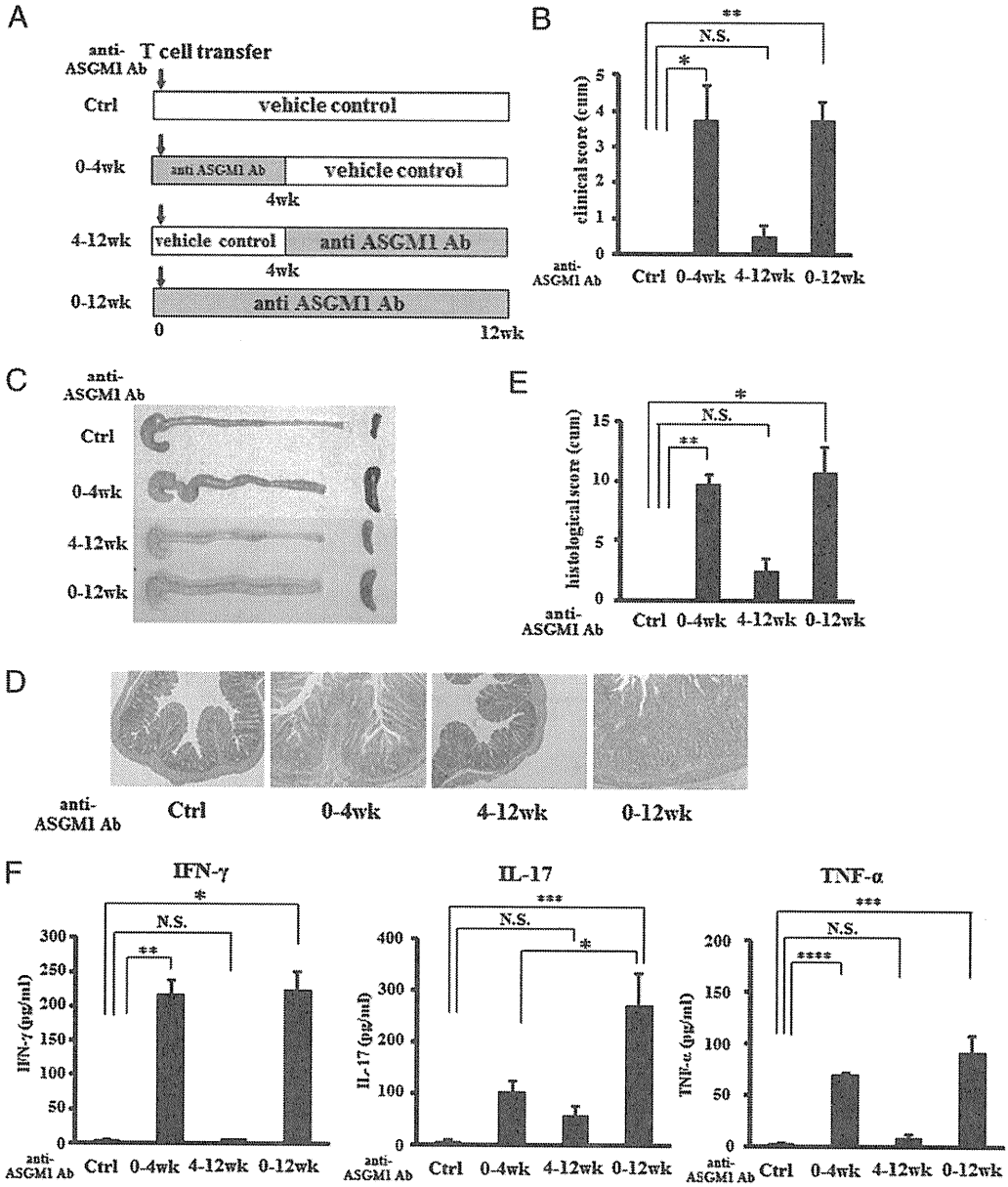

FIGURE 9. NK cell depletion at the early stage, but not at a late stage, in naive T cell-receiving IL-7$^{-/-}$RAG$^{-/-}$ mice results in the elicitation of massive colitis. (**A**) Protocol for NK cell depletion in a setting of chronic colitis. IL-7$^{-/-}$RAG$^{-/-}$ mice were injected with either vehicle control (Ctrl) or anti-ASGM1 Ab (0–12 wk) for 12 wk, anti-ASGM1 Ab for 4 wk followed by vehicle control for 8 wk (0–4 wk), or vehicle control for 4 wk followed by anti-ASGM1 Ab for 8 wk (4–12 wk). (**B**) Clinical scores of each group are shown. Data are expressed as means ± SEM from four mice. *$p < 0.05$, **$p < 0.005$. (**C**) Gross appearance of colons (*left*) and SP (*right*) from naive T cell-transferred IL-7$^{-/-}$RAG$^{-/-}$ recipients injected with either vehicle control for 12 wk (Ctrl), anti-ASGM1 for 4 wk and then vehicle control for 8 wk (0–4 wk), vehicle control for 4 wk and then anti-ASGM1 Ab for 8 wk (4–12 wk), or anti-ASGM1 Ab for 12 wk (0–12 wk). Representative features from four experiments are shown. (**D**) Histological feature of colons from naive T cell-transferred IL-7$^{-/-}$ RAG$^{-/-}$ recipients injected with either control for 12 wk (Ctrl), anti-ASGM1 for 4 wk and then control for 8 wk (0–4 wk), vehicle control for 4 wk and then anti-ASGM1 Ab for 8 wk (4–12 wk), or anti-ASGM1 for 12 wk (0–12 wk). Representative features of each group are shown. (**E**) Histological scores of each group are shown. Data are expressed as means ± SEM from four mice. *$p < 0.05$, **$p < 0.01$. (**F**) Cytokine production by LP T cells from each group is shown. Concentrations of IFN-γ (*left*), TNF (*middle*), and IL-17 (*right*) in the culture supernatant were measured by ELISA. Data are indicated as means ± SEM from four samples. *$p < 0.05$, **$p < 0.01$, ***$p < 0.005$, ****$p < 0.001$.

infiltration in colonic tissues ~4 wk after the adoptive transfer into RAG$^{-/-}$ recipients (10). We therefore compared the effect of NK cell depletion by treatment with an anti-ASGM1 Ab at early (0–4 wk) or late stages (4–12 wk) after naive T cell transfer to treatment over the entire 12-wk period (0–12 wk) after transfer. Ab treatment at the early stage and over the entire 12 wk resulted in a similar degree of colitis exacerbation whereas Ab treatment at the late stage did not exacerbate colitis (Figs. 1, 9). Such exacerbation of colitis occurred relatively latent in the presence of IL-7 in the RAG$^{-/-}$ compared with the IL-7$^{-/-}$RAG$^{-/-}$ recipients when sacrificed at 12 wk after T cell transfer (Figs. 6, 7). However, the difference of colitis severity in the RAG$^{-/-}$ recipients with or without Ab treatment was interestingly remarkable when sacrificed at 6 wk after T cell receiving (Fig. 2). These results imply that NK cell function is critical for colitogenic T cell suppression at the early stage of colitis development.

Because the CD4^{+}CD44^{+}CD62L^{-} colitogenic T_{EM} in the recipients were suggested to be suppressed at the early stage by NK cells (Figs. 1, 2, 9), we further analyzed the effect of NK cells on the development of CD4^{+} T cells within a week after recon-